

THE GLOBAL COLOUR MODEL OF QCD FOR HADRONIC PROCESSES - A REVIEW ¹

Reginald T. Cahill and Susan M. Gunner ²

Department of Physics, Flinders University
GPO Box 2100, Adelaide 5001, Australia

Abstract

The Global Colour Model (GCM) of QCD is a quark-gluon quantum field theory that very successfully models QCD for low energy hadronic processes. An effective gluon correlator models the interaction between quark currents. Functional integral calculus allows the GCM to be hadronised (i.e. expressed in terms of meson and baryon fields). The dominant configuration of the hadronic functional integrals is revealed to be the constituent quark effect, and is identical to one version of the truncated quark Dyson-Schwinger equations (tDSE). However the GCM shows that hadronic physics requires processes that go beyond the tDSE. In this review examples of meson and nucleon processes are given. The GCM also plays a pivotal role in showing how QCD may be related to many other hadronic models

PACS: 12.38.Lg; 13.75.Cs; 11.10.St; 12.38.Aw

Keywords: Quantum Chromodynamics, Global Colour Model, Constituent Quarks, Hadronisation.

¹Published in *Fizika B* **7**(1998)171.

²E-mail: Reg.Cahill@flinders.edu.au, Susan.Gunner@flinders.edu.au

Contents

1	Introduction	2
2	Global Colour Model	3
3	Hadronisation	5
3.1	Meson-Diquark Bosonisation	6
3.2	Baryons	7
3.3	Mesons	10
3.4	Hidden Chiral Symmetry	11
3.5	Hadronic Laws	12
4	Effective Gluon Correlator	13
5	Constituent Quarks	18
6	Constituent Mesons and Diquarks	20
7	Constituent Nambu-Goldstone Mesons	21
8	Constituent Nucleon	25
9	Pion Dressing of Constituent Nucleon	27
10	Connections to Other Models	28
11	Conclusion	29

1 Introduction

We review the Global Colour Model (GCM) (Cahill and Roberts (1985)[1]) of Quantum Chromodynamics (QCD) with particular emphasis on its hadronisation and the resulting applications to low energy meson and nucleon processes. Other reviews of the GCM are Cahill (1989)[2], Cahill (1992)[3], Roberts and Williams (1994)[4], Tandy (1996)[5], Cahill and Gunner (1997)[6] and Tandy (1997)[7]. QCD is defined by the quantisation of the quark-gluon fields with ‘classical’ action $S[\bar{q}, q, A_\mu^a]$. However all evidence for the quarks and gluons is provided by the properties and interactions of the hadrons and by processes involving the electroweak particles. These hadronic laws are encoded in an effective action $S[\pi, \rho, \omega, \dots, \bar{N}, N, .]$, where $\pi(x), \dots, \bar{N}(x), N(x), \dots$ are fields describing composite constituent (equivalently core or bare) hadrons, with ‘centre-of-mass coordinates’ x . These hadronic fields are to be quantised subject to this effective action, yielding finally the observables of QCD. Such an effective action must clearly be non-local because of the composite nature of these hadrons. While a general derivation of $S[\pi, \dots, \bar{N}, N, .]$ from $S[\bar{q}, q, A_\mu^a]$ has not been achieved, it is possible to do this hadronisation within the GCM. The hadronisation uses Functional Integral Calculus (FIC) techniques, which amount to dynamically determined changes of integration variables in the functional integral formulation of the GCM;

$$\int D\bar{q}DqDA \exp(-S_{GCM}[A, \bar{q}, q]) = \int D\pi..D\bar{N}DN.. \exp(-S_{had}[\pi, \dots, \bar{N}, N, .]). \quad (1)$$

Here the constituent hadrons are essentially the normal modes. A particular feature of the GCM is that it plays a pivotal role in relating various seemingly different modellings of QCD as shown in Fig.1, and these relationships will be discussed later. A key task in using the GCM is the determination of the low energy quark-gluon processes from experimental data. In recent years there have

been three such extractions of increasing complexity: GCM95[8], GCM97[9] and GCM98[10]. We report here new detailed *ab initio* studies of the nucleon within the GCM in which one proceeds in a rigorous manner from the experimentally determined low energy quark-gluon processes to detailed dynamical studies of the nucleon, including dressing by the pions.

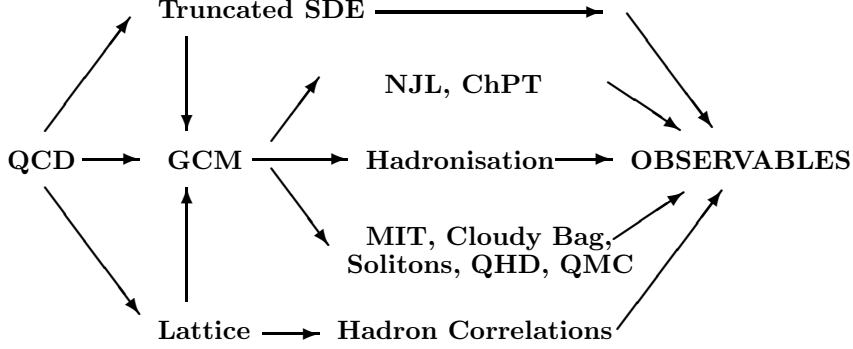


Figure 1: Relational map of the GCM to QCD and various other modellings including the Nambu - Jona-Lasinio (NJL), Quantum Hadrodynamics (QHD), Quark Meson Coupling (QMC) and Chiral Perturbation Theory (ChPT).

2 Global Colour Model

Here we discuss the construction of the GCM from QCD. In the functional integral approach correlators are defined by

$$\mathcal{G}(\dots, x, \dots) = \frac{\int D\bar{q} Dq DAD\bar{C}DC \dots q(x) \dots \exp(-S_{QCD}[A, \bar{q}, q, \bar{C}, C])}{\int D\bar{q} Dq DAD\bar{C}DC \exp(-S_{QCD}[A, \bar{q}, q, \bar{C}, C])} \quad (2)$$

where the ‘classical’ action defining chromodynamics is, in Euclidean metric,

$$\begin{aligned} S_{QCD}[\bar{q}, q, A_\mu^a] = \int d^4x & \left(\frac{1}{4} F_{\mu\nu}^a F_{\mu\nu}^a + \frac{1}{2\xi} (\partial_\mu A_\mu^a)^2 \right. \\ & \left. + \bar{q}(\gamma_\mu - ig \frac{\lambda^a}{2} A_\mu^a) + \mathcal{M} \right) q. \end{aligned} \quad (3)$$

This involves the quark and gluon fields and the field strength tensor for the gluon fields. $\mathcal{M} = \{m_u, m_d, \dots\}$ are the quark current masses, and ghost (\bar{C}, C) and gauge fixing terms must be added to S_{QCD} in (3). The chromodynamic action clearly has two important invariance groups, Poincaré symmetry and the local colour symmetry. The various complete (denoted by scripted symbols) correlators \mathcal{G} lead to experimental observables. They are related by an infinite set of coupled Dyson-Schwinger Equations (DSE), and by the Slavnov-Taylor gauge-symmetry identities and, in the chiral limit, to the axial Ward-Takahashi identity (AWTI). The usual truncation of these DSE causes the violation of all these identities. The correlators in (2) may be extracted from the generating functional of QCD,

$$Z_{QCD}[\bar{\eta}, \eta, J] = \int D\bar{q} Dq DAD\bar{C}DC \exp(-S_{QCD}[A, \bar{q}, q, \bar{C}, C] + \bar{\eta}q + \bar{q}\eta + JA). \quad (4)$$

Functional transformations and approximations lead to the GCM; briefly and not showing source terms for convenience, the gluon and ghost integrations are formally performed

$$\begin{aligned} \int D\bar{q} Dq DAD\bar{C}DC \exp(-S_{QCD}) = \int D\bar{q} Dq \exp(-\int \bar{q}(\gamma \cdot \partial + \mathcal{M})q \\ + \frac{g_0^2}{2} \int j_\mu^a(x) j_\nu^a(y) \mathcal{G}_{\mu\nu}(x-y) + \frac{g_0^3}{3!} \int j_\mu^a j_\nu^b j_\rho^c \mathcal{G}_{\mu\nu\rho}^{abc} + \dots), \end{aligned} \quad (5)$$

where $j_\mu^a(x) = \bar{q}(x) \frac{\lambda^a}{2} \gamma_\mu q(x)$, g_0 is the bare coupling constant, and $\mathcal{G}_{\mu\nu}(x)$ is the gluon correlator with no quark loops but including ghosts (\bar{C}, C)

$$\mathcal{G}_{\mu\nu}(x-y) = \frac{\int DAD\bar{C}DC A_\mu^a(x) A_\nu^a(y) \exp(-S_{QCD}[A, \bar{C}, C])}{\int DAD\bar{C}DC \exp(-S_{QCD}[A, \bar{C}, C])}. \quad (6)$$

Fig.2 shows successive terms in (5). This infinite sequence is a direct consequence of the local non-abelian colour symmetry. The terms of higher order than the term quartic in the quark fields are difficult to explicitly retain in any analysis. The GCM models the effect of higher order terms by replacing the coupling constant g_0 by a momentum dependent quark-gluon coupling $g(s)$, and neglecting terms like $\mathcal{G}_{\mu\nu\rho}^{abc}$ and higher order in (5). This $g(s)$ is a restricted form of vertex function. The modification $g_0^2 \mathcal{G}_{\mu\nu}(p) \rightarrow D_{\mu\nu}(p) = g(p^2) \mathcal{G}_{\mu\nu}(p) g(p^2)$ and the truncation then defines the GCM. We also call this effective quark-quark coupling correlator $D_{\mu\nu}(p)$ the effective gluon correlator and show included processes in Fig.3. As discussed here $D_{\mu\nu}(p)$ may be determined from experimental data. We then formally define the GCM as the quark-gluon field theory with the action

$$S_{GCM}[\bar{q}, q, A_\mu^a] = \int \left(\bar{q}(\gamma \cdot \partial + \mathcal{M} - i A_\mu^a \frac{\lambda^a}{2} \gamma_\mu) q + \frac{1}{2} A_\mu^a D_{\mu\nu}^{-1}(i\partial) A_\nu^a \right) \quad (7)$$

and the generating functional

$$Z[J, \bar{\eta}, \eta] = \int D\bar{q} Dq DA \exp(-S_{GCM}[\bar{q}, q, A_\mu^a] + \bar{\eta}q + \bar{q}\eta + J_\mu^a A_\mu^a). \quad (8)$$

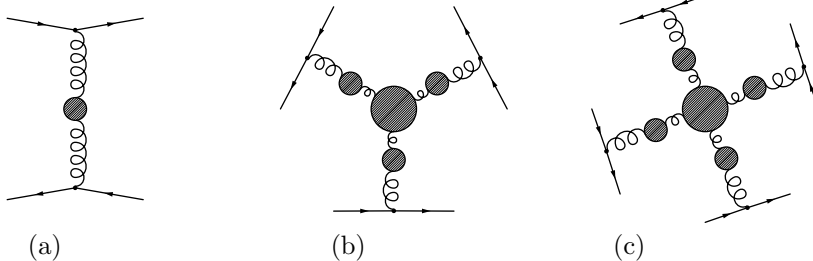


Figure 2: Diagrammatic representation of successive terms in the quark action in (5). The quark-gluon vertex strength is g_0 , while the gluon-gluon vertices (including gluon correlators) are fully dressed except for quark loops.

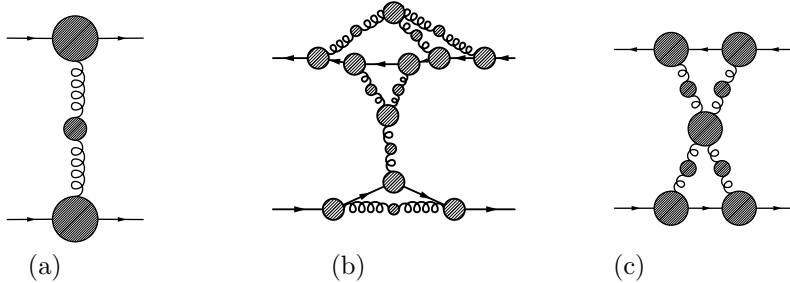


Figure 3: (a) The GCM effective $D_{\mu\nu}$ in (7), (b) example of correlations formally included in (a), and in (c) an $n = 4$ process not formally included in (a), but which is modelled in the GCM via the specific form of $D_{\mu\nu}$.

Here $D_{\mu\nu}^{-1}(p)$ is the matrix inverse of the Fourier transform of $D_{\mu\nu}(x)$. The action S_{GCM} is invariant under $q \rightarrow Uq$, $\bar{q} \rightarrow \bar{q}U^\dagger$ and $A_\mu^a \lambda^a \rightarrow UA_\mu^a \lambda^a U^\dagger$, where U is a global 3×3 unitary colour matrix; this is the global colour symmetry of the GCM. The gluon self-interactions that arise as a consequence of the local colour symmetry in (6) and the ghost and vertex effects lead

to $D_{\mu\nu}^{-1}(p)$ in (7) being non-quadratic. Hence, in effect, the GCM models the QCD local gluonic action $\int F_{\mu\nu}^a[A]F_{\mu\nu}^a[A]$ in S_{QCD} of (2) which has local colour symmetry, by a highly nonlocal action in the last term of (7) which has global colour symmetry. It is important to appreciate that while the GCM has a formal global colour symmetry, the detailed dynamical consequences of the local colour symmetry of QCD are modelled by the particular form of $D(s)$. There is an Infrared (IR) saturation effect which, in conjunction with the dynamical breaking of chiral symmetry, appears to suppress details of the formal colour gauge symmetry of QCD. As well, in the chiral limit $\mathcal{M} \rightarrow 0$, the GCM action has $U_L(N_F) \otimes U_R(N_F)$ symmetry: the $\bar{q} - q$ part of S may be written $\bar{q}\gamma_\mu q = \bar{q}_R\gamma_\mu q_R + \bar{q}_L\gamma_\mu q_L$, where $q_{R,L} = P_{R,L}q$ and $\bar{q}_{R,L} = \bar{q}P_{L,R}$. These two parts are separately invariant under $q_R \rightarrow U_R q_R$, $\bar{q}_R \rightarrow \bar{q}_R U_R^\dagger$ and $q_L \rightarrow U_L q_L$, $\bar{q}_L \rightarrow \bar{q}_L U_L^\dagger$.

A key feature of the GCM analysis is the demonstration that this effective gluon correlator $D_{\mu\nu}(p)$ is successful for a variety of hadronic processes, i.e. it is a *universal* feature of low energy hadronic processes. The success of the GCM appears to be based on the phenomenon of an IR saturation mechanism in which the extreme IR strength of the many contributing quark-quark couplings is easily modelled by this one effective gluon correlator. This was used in the context of the truncated Dyson-Schwinger (tDSE) approach by Munczek and Nemirovsky [11] who used a delta-function form. Of particular dynamical interest is the comparison of the GCM $D_{\mu\nu}(p)$ with one constructed theoretically from only a gluon correlator and vertex functions, say from continuum or lattice modellings, for this gives some insight into the IR strength of the higher order gluonic couplings.

3 Hadronisation

Hadronisation is a generalisation of the bosonisation concept to include the fermionic (baryonic) states. Bosonisation is naturally and conveniently induced using the FIC methods, and indeed the GCM is a spinor-boson field theory which may be exactly bosonised in 4-dimensional spacetime. A key feature of the GCM bosonisation is the use of bilocal fields which simply indicates that the complete theory is expressible using two-point correlators as an equivalent set of functional integration variables. As we shall see the bilocal bosonisation (which precedes the hadronisation) not only generates the mesonic effective action, but also carries structural information which is essential in understanding the couplings of these mesons. This information (i.e. vertex functions) is essential to the prediction of hadronic properties and interactions. If we throw away this emergent information we are left with a non-renormalisable effective field theory with no predictive properties. There are two alternative first stage bosonisations of the GCM. The first in 1985 in which Cahill and Roberts[1] introduced colour singlet and colour octet mesonic correlations had two problems: (a) the colour octet correlations did not appear to have any clear physical significance, and (b) the baryonic states were not manifest. However in 1989 Cahill, Praschifka and Burden[12] discovered a meson-diquark bosonisation which was induced by new colour and Dirac-spinor Fierz identities and which involved the colour singlet mesonic states and the colour $\bar{\mathbf{3}}(qq)$ and $\mathbf{3}(\bar{q}\bar{q})$ diquark/anti-diquark states, these being the very colour subcorrelations present in colour singlet baryons and anti-baryons. The meson-diquark bosonisation then led to the meson-baryon hadronisation of the GCM (Cahill 1989) [13]. This hadronisation automatically produced the covariant Faddeev formulation of the constituent baryon states, and also the meson dressing of these states; see later sections. In this review we concentrate mainly on this modern hadronisation of the GCM, which is summarised by the following sequence of FIC transformations:

$$\begin{aligned}
Z &= \int D\bar{q}DqDA \exp(-S_{QCD}[A, \bar{q}, q] + \bar{\eta}q + \bar{q}\eta) \\
&\approx \int D\bar{q}DqDA \exp(-S_{GCM}[A, \bar{q}, q] + \bar{\eta}q + \bar{q}\eta) \quad (\text{GCM}) \\
&= \int DBD\bar{D}DD \exp(-S[\mathcal{B}, \bar{\mathcal{D}}, \mathcal{D}]) \quad (\text{bilocal fields})
\end{aligned} \tag{9}$$

$$= \int D\bar{N}DN..D\pi D\rho D\omega \dots \exp(-S_{had}[\bar{N}, N, \dots, \pi, \rho, \omega, \dots]) \quad (\text{local fields}). \quad (10)$$

The basic insights are that (i) the quark-gluon dynamics in (2) is fluctuation dominated, whereas the hadronic functional integrations in (10) are not, (ii) the bilocal stage in (9) produces the constituent quark effect as the dominant configuration, and (iii) this entails the IR saturation effect and the dynamical breaking of chiral symmetry and its significant consequences, and (iv) the induced hadronic effective action in (10) is nonlocal. The hadronisation has also been further studied in [14, 15, 16, 17, 18, 19]

3.1 Meson-Diquark Bosonisation

Here we review the meson-diquark bosonisation [2] of the GCM, giving (9). The FIC techniques amount to analogues of various ‘tricks’ of ordinary integral calculus. Integrating out the gluon fields Z becomes,

$$Z[\bar{\eta}, \eta] = \int D\bar{q}Dq \exp\left(-S[\bar{q}, q] + \bar{\eta}q + \bar{q}\eta\right), \quad (11)$$

where

$$S[\bar{q}, q] = \int \left(\bar{q}(x)(\gamma \cdot \partial_x + \mathcal{M})\delta^4(x-y)q(y) + \frac{1}{2}\bar{q}(x)\frac{\lambda^a}{2}\gamma_\mu q(x)D_{\mu\nu}^{ab}(x-y)\bar{q}(y)\frac{\lambda^b}{2}\gamma_\nu q(y) \right). \quad (12)$$

Using the new Fierz identities [12] the quartic term in (12) is rearranged to give

$$\begin{aligned} S[\bar{q}, q] = & \int d^4x d^4y \left[\bar{q}(x)\gamma \cdot \partial \delta^4(x-y)q(y) - \frac{1}{2}\bar{q}(x)\frac{M_m^\theta}{2}q(y)D(x-y) \right. \\ & \left. \cdot \bar{q}(y)\frac{M_m^\theta}{2}q(x) - \frac{1}{2}\bar{q}(x)\frac{M_d^\phi}{2}\bar{q}(y)^{cT}D(x-y)q(y)^{cT}\frac{M_d^\phi}{2}q(x) \right], \end{aligned} \quad (13)$$

with $q^c = Cq$, $\bar{q}^c = \bar{q}C$. The Fierz identities are the two Dirac matrix identities $\gamma_{rs}^\mu \gamma_{tu}^\mu = K_{ru}^a K_{ts}^a$ where $\{K^a\} = \{\mathbf{1}, i\gamma_5, \frac{i}{\sqrt{2}}\gamma^\mu, \frac{1}{\sqrt{2}}\gamma^\mu\gamma_5\}$, and $\gamma_{rs}^\mu \gamma_{tu}^\mu = (K^a C^T)_{rt}(C^T K^a)_{us}$ where $C = \gamma^2\gamma^4$, $C^2 = -\mathbf{1}$ and $C\gamma^\mu C = \gamma^{\mu T}$. We also use the set $\{\bar{K}^a\} = \{\mathbf{1}, -i\gamma_5, \frac{-i}{2\sqrt{2}}\gamma^\mu, \frac{1}{2\sqrt{2}}\gamma^\mu\gamma_5\}$, then $tr[\bar{K}^a K^b] = 4\delta_{ab}$. For the colour algebra [12] $\lambda_{\alpha\beta}^a \lambda_{\gamma\delta}^a = \frac{4}{3}\delta_{\alpha\delta}\delta_{\beta\gamma} + \frac{2}{3}\sum_{\rho=1}^3 \epsilon_{\rho\alpha\gamma}\epsilon_{\rho\delta\beta}$, while for the $N_f = 3$ flavour algebra, $\delta_{ij}\delta_{kl} = F_{il}^c F_{kj}^c$ for the mesons where $\{F^c, c = 0, \dots, 8\} = \{\frac{1}{\sqrt{3}}\mathbf{1}, \frac{\lambda^1}{\sqrt{2}}, \dots, \frac{\lambda^8}{\sqrt{2}}\}$ and $\delta_{ij}\delta_{kl} = H_{ik}^f H_{lj}^f$ for the diquarks, where $\{H^f, f = 1, \dots, 9\} = \{F^c, c = 7, 5, 2, 0, 1, 3, 4, 6, 8\}$ and where $\{\frac{\lambda^a}{2}\}$ are the generators of $SU(3)$ in the usual Gell-Mann representation. We define the tensor products $\{M_m^\theta\} = \{\sqrt{\frac{4}{3}}K^a F^c\}$ and $\{M_d^\phi\} = \{i\sqrt{\frac{2}{3}}K^a \epsilon^\rho H^f\}$, where $(\epsilon^\rho)_{\alpha\beta} = \epsilon_{\rho\alpha\beta}$. We see that $\bar{q}(y)M_m^\theta q(x)$ are $\mathbf{1}_c$ bilocal $\bar{q}q$ fields with the flavour ($\mathbf{1}_f$ or $\mathbf{8}_f$) determined by the flavour generators ($\{F^0\}$ or $\{F^{1, \dots, 8}\}$) in M_m^θ , while $q(y)^{cT}M_d^\phi q(x)$ are $\bar{\mathbf{3}}_c$ bilocal qq fields with the flavour ($\bar{\mathbf{3}}_f$ or $\mathbf{6}_f$) determined by the flavour generators ($\{H^{1,2,3}\}$ or $\{H^{4, \dots, 9}\}$) in M_d^ϕ . These results follow from the colour and flavour representation of the quark fields. The (integral) spin of these boson fields is determined by the K^a . By rewriting (12) as (13) we can initiate a bosonisation which is adapted to the attractive channels implicit in (12). The 1985 GCM colour Fierz identity [1] leads to the colour $\mathbf{8}$ channels which are repulsive.

We make the first FIC change of variables by noting that the quartic terms in $\exp(-S)$ may be generated by the following bilocal FIC integrations,

$$\begin{aligned} Z = & \int D\bar{q}Dq D\mathcal{B} D\mathcal{D} D\mathcal{D}^* \exp\left(\int \left[-\bar{q}(x)(\gamma \cdot \partial + \mathcal{M})\delta^4(x-y)q(y) \right. \right. \\ & \left. \left. - \frac{\mathcal{B}^\theta(x, y)\mathcal{B}^\theta(y, x)}{2D(x-y)} - \frac{\mathcal{D}^\phi(x, y)\mathcal{D}^\phi(x, y)^*}{2D(x-y)} \right] \right. \end{aligned}$$

$$\begin{aligned}
& -\bar{q}(x) \frac{M_m^\theta}{2} q(y) \mathcal{B}^\theta(x, y) - \frac{1}{2} \bar{q}(x) \frac{M_d^\phi}{2} \bar{q}(y) {}^{cT} \mathcal{D}^\phi(x, y)^\star \\
& - \frac{1}{2} \mathcal{D}^\phi(x, y) q(y) {}^{cT} \frac{M_d^\phi}{2} q(x) \Big] + \int (\bar{\eta} q + \bar{q} \eta) \Big),
\end{aligned} \tag{14}$$

where $\mathcal{B}^\theta(x, y) = \mathcal{B}^\theta(y, x)^\star$ are ‘hermitean’ bilocal fields. Integration over the quark fields completes the change of variables to bilocal meson and diquark fields,

$$\begin{aligned}
Z[\bar{\eta}, \eta] = & \int D\mathcal{B} D\mathcal{D} D\mathcal{D}^\star (Det \mathcal{F}^{-1}[\mathcal{B}, \mathcal{D}, \bar{\mathcal{D}}])^{\frac{1}{2}} \exp \left(\int -\frac{\mathcal{B}^\theta(x, y) \mathcal{B}^\theta(y, x)}{2D(x-y)} \right. \\
& \left. - \int \frac{\mathcal{D}^\phi(x, y) \mathcal{D}^\phi(x, y)^\star}{2D(x-y)} + \frac{1}{2} \int \Theta \mathcal{F} \Theta^T \right),
\end{aligned} \tag{15}$$

$$\text{where } \Theta \equiv (\bar{\eta}, -\eta^T), \quad \mathcal{F}^{-1}[\mathcal{B}, \mathcal{D}, \bar{\mathcal{D}}] = \begin{pmatrix} -\mathcal{D} & G^{-1T} \\ -G^{-1} & -\bar{\mathcal{D}} \end{pmatrix},$$

$$G^{-1}(x, y, \mathcal{B}) = (\gamma \cdot \partial + \mathcal{M}) \delta^4(x-y) + \mathcal{B}(x, y), \quad \mathcal{B}(x, y) = \mathcal{B}^\theta(x, y) \frac{M_m^\theta}{2}, \tag{16}$$

$$\bar{\mathcal{D}}(x, y) = \mathcal{D}^\phi(x, y)^\star \frac{M_d^\phi}{2} C^T \quad \text{and} \quad \mathcal{D}(x, y) = \mathcal{D}^\phi(y, x) C^T \frac{M_d^\phi}{2}.$$

Using the determinant identity [12] $Det \mathcal{F}^{-1} = (Det(G^{-1}))^2 Det(\mathbf{1} + \bar{\mathcal{D}} G^T \mathcal{D} G)$,

$$\begin{aligned}
Z = & \int D\mathcal{B} D\mathcal{D} D\mathcal{D}^\star \exp \left(Tr Ln(G[\mathcal{B}]^{-1}) + \frac{1}{2} Tr Ln(\mathbf{1} + \bar{\mathcal{D}} G[\mathcal{B}]^T \mathcal{D} G[\mathcal{B}]) + \right. \\
& \left. - \int \frac{\mathcal{B}^\theta \mathcal{B}^{\theta\star}}{2D} - \int \frac{\mathcal{D}^\phi \mathcal{D}^{\phi\star}}{2D} + \frac{1}{2} \int \Theta \mathcal{F} \Theta^T \right).
\end{aligned} \tag{17}$$

3.2 Baryons

The diquark sector of the meson-diquark bosonisation generates [2] the colour singlet baryon states of the GCM. Consider the diquark part of Z ;

$$Z = \int D\mathcal{D} D\mathcal{D}^\star \exp \left(\frac{1}{2} Tr Ln(\mathbf{1} + \bar{\mathcal{D}} G^T \mathcal{D} G) - \int \frac{\mathcal{D} \mathcal{D}^\star}{2D} + \int (J^\star \mathcal{D} + \mathcal{D}^\star J) \right),$$

where the bilocal diquark source terms facilitate the analysis, and in which the \mathcal{B} dependence of $G[\mathcal{B}]$ will affect both the non-trivial dominant configuration and the mesons, and will provide the meson-baryon couplings. The expansion

$$Tr Ln(\mathbf{1} + \bar{\mathcal{D}} G^T \mathcal{D} G) = \sum_{n=1}^{\infty} \frac{(-1)^{(n+1)}}{n} Tr(\bar{\mathcal{D}} G^T \mathcal{D} G)^n, \tag{18}$$

gives single loop processes (Fig.4(a)) with the quark lines alternating in direction, in accord with their coupling to the diquark and anti-diquark fields. Using (18) the diquark part of the action has the expansion $S[\mathcal{D}^\star, \mathcal{D}] = \sum_n S_n[\mathcal{D}^\star, \mathcal{D}]$ and with $S_1 = \int \mathcal{D}^{\phi\star} (\Delta_d^{-1})^{\phi\psi} \mathcal{D}^\psi$ and $S' = S - S_1$,

$$\begin{aligned}
Z = & \exp(-S'[\frac{\delta}{\delta J^\star}, \frac{\delta}{\delta J}]) \int D\mathcal{D} D\mathcal{D}^\star \exp \left(- \int \mathcal{D}^\star \Delta_d^{-1} \mathcal{D} + \int (J^\star \mathcal{D} + \mathcal{D}^\star J) \right) \\
= & \exp(-S'[\frac{\delta}{\delta J^\star}, \frac{\delta}{\delta J}]) \exp \left(-Tr Ln(\Delta_d^{-1}) + \int J^\star \Delta_d J \right).
\end{aligned} \tag{19}$$

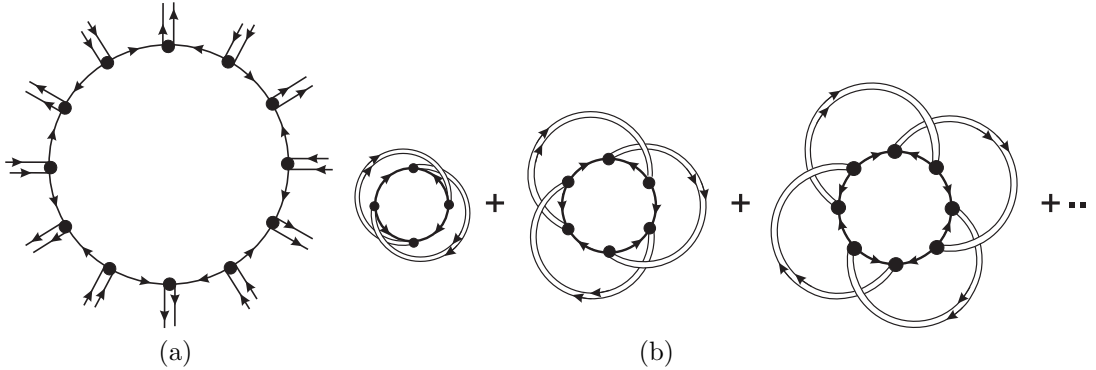


Figure 4: (a) Example of diagrams from expansion of diquark $TrLn$ in (18). (b) Diagrams after diquark field integrations.

Keeping only the translation invariant part of $\mathcal{B}, \mathcal{B}_{CQ}(x-y)$ - later to be identified as the constituent quark (CQ) effect, Δ_d^{-1} has eigenvalues and eigenvectors (diquark form factors) from

$$\int \frac{d^4 q}{(2\pi)^4} (\Delta_d^{-1})^{\phi\psi}(p, q; P) \Gamma_k^\psi(q; P) = \lambda_k(P^2) \Gamma_k^\phi(p; P) \quad (20)$$

and we have the orthonormality, completeness and spectral equations

$$\sum_\theta \int \frac{d^4 q}{(2\pi)^4} \Gamma_k^\theta(q; P)^* \Gamma_l^\theta(q; P) = \delta_{kl}, \quad \sum_k \Gamma_k^\theta(q; P) \Gamma_k^\phi(p; P)^* = (2\pi)^4 \delta_{\theta\phi} \delta^4(q-p),$$

$$\Delta_d^{\phi\psi}(p, q; P) = \sum_k \Gamma_k^\phi(p; P) \lambda_k(P^2)^{-1} \Gamma_k^\psi(q; P)^*. \quad (21)$$

Using completeness we construct the local-diquark-field FIC representation

$$TrLn(\Delta_d^{-1}) = \sum_k \int d^4 x \int \frac{d^4 P}{(2\pi)^4} \ln(\lambda_k(P^2)) = \sum_k TrLn(\lambda_k(-\partial^2) \delta^4(x-y)), \quad (22)$$

$$\exp(-TrLn(\Delta_d^{-1})) = \int Dd_k Dd_k^* \exp\left(-\sum_k \int d_k(x)^* \lambda_k(-\partial^2) \delta^4(x-y) d_k(y)\right). \quad (23)$$

Introducing local sources $j_k(X) = \int d^4 Y d^4 x \Gamma_k^\phi(x, X-Y)^* J^\phi(x, Y)$, so that

$$\frac{\delta}{\delta J^\phi(x, X)} = \sum_k \int d^4 Y \Gamma_k^\phi(x, Y-X)^* \frac{\delta}{\delta j_k(Y)},$$

but keeping only a single component of the scalar diquark to simplify notation,

$$Z[j^*, j] = \exp\left(-S'[\frac{\delta}{\delta j^*}, \frac{\delta}{\delta j}]\right) \exp\left(-TrLn(\Delta_d^{-1}) + \int j^*(X) \lambda_0(-\partial^2)^{-1} j(X)\right). \quad (24)$$

Evaluating the effect of the functional operator we find that $Z[0, 0]$ has the form $\exp(W)$ where W is the sum of connected loop diagrams, with the vertices now joined by the diquark correlators $\lambda_0(P^2)^{-1} = (P^2 + m_0(P^2)^2) f^2$, in which $m_0(P^2)$ is the diquark mass function, and with $\Gamma_0(p; P)$ at the vertices. Of particular significance is the infinite subset of diagrams which will be seen to have the form of three-quark (i.e. baryon) loops (Fig.5(a)). These come with a combinatoric factor of 2 (except for the order $n=3$ diagram) which cancels the $\frac{1}{2}$ coefficient of the $TrLn$. These 3-loops are planar for even order, but non-planar, with one twist, for odd order. To exhibit the three-quark loop structure we show, in Fig.5(a), a typical diagram from Fig.4(b) after deformation, revealing a

closed double helix: a diagram of order n is drawn on a Möbius strip of $n - 1$ twists. This infinite series may be summed as the diagrams are generated by the kernel K , defined by the one-twist diagram, shown in Fig.5(b).

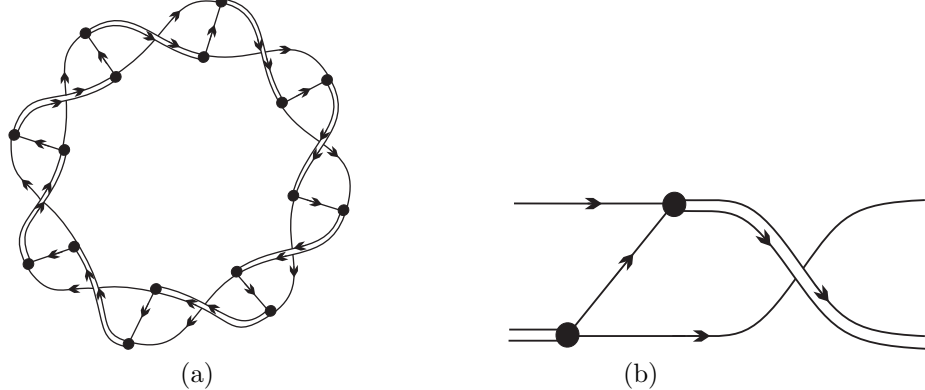


Figure 5: (a) Similar to Fig.4(b) after redrawing to reveal baryon loop. These loop functionals determine the core baryon mass spectrum. (b) Kernel of the nucleon loop.

The weightings are such that all the double helix diagrams may be summed to $\text{Tr} \ln(\mathbf{1} + K) - \text{Tr} K = W_B - \text{Tr} K$. Thus $Z[0,0] = \exp(W_B + D_R)$, in which D_R is the sum of the remaining connected diagrams. To determine the content of W_B we consider the eigenvalue problem $(\mathbf{1} + K)\Psi = \lambda\Psi$, which, for $\mathcal{B} = \mathcal{B}_{CQ}$, has the following momentum space form, and is illustrated in Fig.6

$$\int \frac{d^4q}{(2\pi)^4} K(p, q; P)_{\alpha f, \gamma l}^{\beta j, \rho h} \Psi_{\rho h}^{\gamma l}(q; P) = (\lambda(P^2) - 1) \Psi_{\alpha f}^{\beta j}(p; P), \quad (25)$$

$$K(p, q; P)_{\alpha f, \gamma l}^{\beta j, \rho h} = \sum_{i\delta} \frac{1}{12} \Gamma_0 \epsilon_{\gamma\alpha\delta} \epsilon_{l f i} i\gamma_5 C^T G^T C^T i\gamma_5 \epsilon_{\beta\delta\rho} \epsilon_{j i h} \Gamma_0 G \lambda_0^{-1}. \quad (26)$$

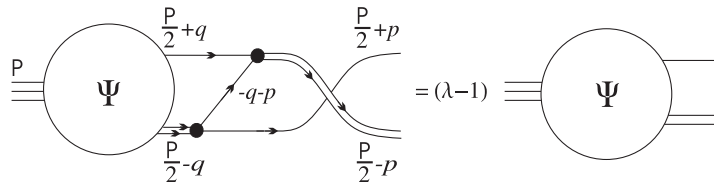


Figure 6: The core baryon eigenvector equation. The diquark vertex is shown shaded. The diquark is essentially the same size as the baryon.

Equation (25) is a bound state equation for a three-quark state in which the paired quarks form a scalar diquark. Ψ in (25) is a Dirac spinor and, as well, a rank-2 tensor in both colour and flavour. It should also be clear why the baryon loop functional consists of twisted quark-diquark lines; (25) is precisely of the form of the Faddeev equations of standard three-particle theory - the twisting merely arose so that the diagrammatic representation of (25) in Fig.6 has the same legs in the same positions on both sides of the equation; conventionally Fig.6 would be drawn in untwisted form. In fact (25) was also derived by conventional non-FIC three-particle methods [2]. See [20, 21] for early quark-diquark models. We note that because (21) is a discrete sum, (25) is of separable form. We separate colour and flavour multiplets in (25), by decomposing $\Psi_{\rho h}^{\gamma l}$ according to $(\mathbf{3} \otimes \bar{\mathbf{3}})_C \otimes (\mathbf{3} \otimes \bar{\mathbf{3}})_F = (\mathbf{1}_C \otimes \mathbf{1}_F) \oplus (\mathbf{1}_C \otimes \mathbf{8}_F) \oplus (\mathbf{8}_C \otimes \mathbf{1}_F) \oplus (\mathbf{8}_C \otimes \mathbf{8}_F)$,

$$\Psi_{\rho h}^{\gamma l} = \frac{1}{9} \delta_{\gamma\rho} [\Psi_{\alpha k}^{\alpha k}] \delta_{lh} + \frac{1}{3} \delta_{\gamma\rho} [\Psi_{\alpha h}^{\alpha l} - \frac{1}{3} \Psi_{\alpha k}^{\alpha k} \delta_{lh}] +$$

$$+ \frac{1}{3}[\Psi_{\rho k}^{\gamma k} - \frac{1}{3}\Psi_{\alpha k}^{\alpha k}\delta_{\gamma\rho}]\delta_{lh} + [\Psi_{\rho h}^{\gamma l} - \frac{1}{3}\Psi_{\alpha h}^{\alpha l}\delta_{\rho\gamma} - \frac{1}{3}\Psi_{\rho k}^{\gamma k}\delta_{lh} + \frac{1}{9}\Psi_{\alpha k}^{\alpha k}\delta_{\gamma\rho}\delta_{lh}]. \quad (27)$$

Each member ($\Psi \equiv [...]$) of one multiplet is then seen to be an eigenvector of

$$\int \frac{d^4 q}{(2\pi)^4} K(p, q; P) \Psi(q; P) = (\lambda(P^2) - 1) \Psi(p; P), \quad (28)$$

$$K(p, q; P) = -\frac{N[m]}{6} \Gamma_0\left(\frac{P}{4} + q + \frac{p}{2}; \frac{P}{2} - p\right) \Gamma_0\left(\frac{P}{4} + p + \frac{q}{2}; \frac{P}{2} - q\right) \cdot \lambda_0\left(\left(\frac{P}{2} - q\right)^2\right)^{-1} G(-q - p) G\left(\frac{P}{2} + q\right), \quad (29)$$

where the $N[m]$ depend on the multiplet, and we find $N[\mathbf{1}_C \otimes \mathbf{1}_F] = -2$, $N[\mathbf{1}_C \otimes \mathbf{8}_F] = +1$, $N[\mathbf{8}_C \otimes \mathbf{1}_F] = +1$ and $N[\mathbf{8}_C \otimes \mathbf{8}_F] = -\frac{1}{2}$. The $\mathbf{1}_C \otimes \mathbf{1}_F$ and $\mathbf{8}_C \otimes \mathbf{8}_F$ multiplets have negative values for N and thus the quark rearrangement process is repulsive, and the corresponding $\lambda(-M^2)$'s have no zeros. However the colour octet - flavour singlet 'baryons' have an N value which means they are degenerate in mass with the colour-singlet flavour-octet baryons. Like the diquark states we expect colour non-singlets to not have a mass-shell, i.e. to be confined. It is known that crossed gluon processes can perform this task for the diquarks[22] (see sect.6), but there has been no corresponding analysis for these coloured baryonic states.

Let us now construct, for the colour singlet states, an appropriate FIC representation for $\exp(TrLn(\mathbf{1} + K))$. To this end note that an eigenvalue for positive energy solutions, with degeneracy 2 (for spin \uparrow and \downarrow), has the form $\lambda_+^{\uparrow\downarrow}(P^2) = (M(P^2) + i\sqrt{P^2 a(P^2)})F$, (define F so that $a = 1$ when $\lambda = 0$, then $M_k(P^2)$ are baryon running masses), while for negative energy solutions (anti-baryons) $\lambda_-^{\uparrow\downarrow} = (\lambda_+^{\uparrow\downarrow})^*$. Thus, from the spectral representation for $\mathbf{1} + K$,

$$\exp(TrLn(\mathbf{1} + K)) = \exp\left(\sum_k n \int d^4 x \int \frac{d^4 P}{(2\pi)^4} [ln(\lambda_+^{\uparrow\downarrow}(P^2)^2) + ln(\lambda_-^{\uparrow\downarrow}(P^2)^2)]\right) \quad (30)$$

where k sums the ground state and excited baryons states of (25), the squares in the ln terms arise from the spin degeneracy and $n = 8$ arises from the flavour degeneracy (the other baryon states are not shown). Therefore, with $a = 1$ for simplicity,

$$\begin{aligned} \exp(TrLn(\mathbf{1} + K)) &= \exp\left(\sum_k n \int d^4 x \int \frac{d^4 P}{(2\pi)^4} ln\left[(P^2 + M_k(P^2)^2)^2 F_k^4\right]\right) \\ &= \exp\left(\sum_k TrLn\left[(\gamma \cdot \partial + M_k(-\partial^2))F_k^2 \delta^4(x - y)\right]\right) \\ &= \int D\bar{N}_k DN_k \exp\left(-\sum_k \int d^4 x \bar{N}_k(x) (\gamma \cdot \partial + M_k(-\partial^2))F_k^2 N_k(x)\right), \end{aligned} \quad (31)$$

in terms of \bar{N}_k and N_k , each of which is a flavour octet of local baryonic spin $\frac{1}{2}$ FIC variables. Hence the exponentiated sum of the closed double helix diagrams is representable as a (free) baryon field theory. The F_k may be absorbed with a re-definition of the baryon fields. Other more complicated (including baryon multi-loops) diagrams are present and constitute a wealth of dressings and interactions between these (bare) baryons.

3.3 Mesons

We now briefly indicate how the non-diquark part of (17), $S[\mathcal{B}]$, gives the meson sector. The complete Z has the form

$$Z = \int D\mathcal{B} \exp\left(-S[\mathcal{B}] - \sum_{diquarks} TrLn(\lambda_k(-\partial^2; [\mathcal{B}_{CQ}])\delta^4(x - y))\right)$$

$$+ \sum_{baryons} TrLn((\gamma \cdot \partial + M_k(-\partial^2; [\mathcal{B}_{CQ}]))\delta^4(x-y)) + \Big). \quad (32)$$

We first determine the dominant configuration (and constituent quark effect) \mathcal{B}_{CQ} , as the solution of the Euler-Lagrange equations $\frac{\delta[S+..]}{\delta\mathcal{B}^\theta} = 0$, which gives

$$\mathcal{B}_{CQ}^\theta(x, y) = D(x-y) \left[\text{tr}(G(x, y, \mathcal{B}_{CQ}) \frac{M_m^\theta}{2}) + \right], \quad (33)$$

a non-linear equation for the $\{\mathcal{B}_{CQ}^\theta\}$. - a Dyson-Schwinger type equation, where ‘+....’ are the diquark and baryon parts. Dynamically it describes the extensive self-energy of the quarks due to dressing by gluons, leading to the quark running mass. This is finite and extends over distances comparable to hadronic sizes and with an energy density that implies that it has the dominant role in determining hadron structure. Only colour-singlet translation-invariant solutions (depending only on $x-y$) are known. Fourier and inverse Fierz transforming (33) we obtain, on retaining only the meson contributions,

$$\mathcal{B}_{CQ}(p) = c \cdot \frac{4}{3} \int \frac{d^4 q}{(2\pi)^4} D(p-q) \gamma_\mu \frac{1}{i\gamma \cdot q + \mathcal{M} + \mathcal{B}_{CQ}(q)} \gamma_\mu. \quad (34)$$

Here $c = \frac{3}{4}$ from the meson-diquark bosonisation, while normal Feynman rules would give $c = 1$, as does the **1 – 8** GCM bosonisation [1]. That $c < 1$ in the **1 – 3 – 3** bosonisation indicates that some strength is generated by additional mechanisms in (33) involving meson and diquark processes, i.e. the ‘book-keeping’ is more subtle in this bosonisation, and is so to avoid double counting. At present we adopt the practice of using $c = 1$ until these additional processes can be included dynamically. This CQ equation has unique solutions when $\mathcal{M} \neq 0$ and G has the form $G(q) = [iA(q)q \cdot \gamma + \mathcal{M} + B(q)]^{-1}$. Expanding $S[\mathcal{B}]$ about its minimum gives $S[\mathcal{B}] = \sum_{n=0,2,3..} S_n[\mathcal{B}]$, where S_n is of order n in \mathcal{B} and, for example, $S_2 = \frac{1}{2} \int \mathcal{B}^\theta (\Delta_m^{-1})^{\theta\psi} \mathcal{B}^\psi$. Introducing bilocal source terms in (32) we have, with $S' = S - S_2$, and showing only the meson part,

$$\begin{aligned} Z[J] &= \int D\mathcal{B} \exp(-S'[\mathcal{B}] - S_2[\mathcal{B}] + \int \mathcal{B}^\theta J^\theta) \\ &= \exp(-S'[\frac{\delta}{\delta J}]) \int D\mathcal{B} \exp(-\int \frac{1}{2} \mathcal{B}^\theta (\Delta_m^{-1})^{\theta\psi} \mathcal{B}^\psi + \int \mathcal{B}^\theta J^\theta), \\ &= \exp(-S'[\frac{\delta}{\delta J}]) \int Dm_k \exp(-\sum_k \frac{1}{2} \int m_k(x) \lambda_k(-\partial^2) m_k(x) + \int j_k m_k). \end{aligned}$$

Here we have used techniques similar to that for the diquarks and $\{m_k(x)\}$ is an infinite set of local meson fields. Each m_k corresponds to one physical meson type, and the λ_k are the eigenvalues of the meson form of (20)- a Bethe-Salpeter equation, which also gives the meson form factors $\Gamma_k(p, P)$. Applying the functional operator $\exp(-S'[\frac{\delta}{\delta J}])$,

$$Z = \int Dm_k \exp \left(-\sum_k \frac{1}{2} \int m_k(x) \lambda(-\partial^2) m_k(x) - S'[m_k] \right). \quad (35)$$

By evaluation of $S'[m_k]$, and identifying the mesons by their quantum numbers, we obtain the full local FIC representation for the meson sector of QCD [2, 23, 24], as summarised in sect. 3.5.

3.4 Hidden Chiral Symmetry

When the quark current masses $\mathcal{M} \rightarrow 0$ the fundamental action $S[\bar{q}, q, A_\mu^a]$ has the important additional global $U_L(N_F) \otimes U_R(N_F)$ chiral symmetry. The consequences of this follow naturally

through the GCM hadronisation. The first significant result is that the dominant configuration (34) has degenerate solutions [1, 2, 25]

$$G(q; V) = [iA(q)q \cdot \gamma + VB(q)]^{-1} = \zeta^\dagger G(q; \mathbf{1})\zeta^\dagger, \quad (36)$$

where $\zeta = \sqrt{V}$, $V = \exp(i\sqrt{2}\gamma_5\pi^a F^a)$ and $\{\pi^a\}$ are arbitrary real constants $|\pi| \in [0, 2\pi]$. Thus in the chiral limit the dominant configuration is degenerate and is the manifold $(U_L \otimes U_R)/H$ (a coset space) where $H = U_V \subset U_L \otimes U_R$. Thus the chiral symmetry is represented as a hidden symmetry. This occurs because the action in (32) has the form of a ‘Mexican-hat’ in the relevant variables [2]. The Nambu-Goldstone (NG) bosons form homogeneous Riemann coordinates for this dominant configuration manifold. There is a technical complexity in expanding $S'[m_k]$ in the chiral limit which is caused by the action having degenerate minima, since we do not have a unique minimum about which to expand. First we need fields adapted to the compact dominant configuration manifold. For this we use the angles $\{\pi\}$ as new field variables $\{\pi(x)\}$ [25, 26] in place of some of the $\mathcal{B}^\theta(x, y)$. The dependence of the action on these dominant configuration variables is such that the action will increase only if the dominant configuration point is different at different space-time points, and so a derivative expansion in $\partial_\mu V(x)$ must arise. The Dirac algebra allows finally the use of the matrix $U(x) = \exp(i\sqrt{2}\pi^a(x)F^a)$ where $V(x) = P_L U(x)^\dagger + P_R U(x) = \exp(i\sqrt{2}\gamma_5\pi^a(x)F^a)$. Then the NG sector of $S[\mathcal{B}]$ is

$$\begin{aligned} \int d^4x \left(\frac{f_\pi^2}{4} \text{tr}(\partial_\mu U \partial_\mu U^\dagger) + \kappa_1 \text{tr}(\partial^2 U \partial^2 U^\dagger) + \kappa_2 \text{tr}([\partial_\mu U \partial_\mu U^\dagger]^2) \right. \\ \left. + \kappa_3 \text{tr}(\partial_\mu U \partial_\nu U^\dagger \partial_\mu U \partial_\nu U^\dagger) + \frac{\rho}{2} \text{tr}([\mathbf{1} - \frac{U + U^\dagger}{2}] \mathcal{M}) + \dots \right) \end{aligned} \quad (37)$$

where f_π, κ_1, \dots are given by explicit integrals [25, 26] in terms of $A(q)$ and $B(q)$ and ρ is the quark condensate parameter. In the chiral limit it is important to note [2, 25] that $B(q)$ in the quark correlator is also the NG boson on-mass-shell form factor, $\Gamma_\pi(p; \mathbf{P} = \mathbf{0}) = B(p)$. In the chiral limit the ground state pseudoscalars play a dual role: they are at the same time both the NG bosons associated with the hidden chiral symmetry and also $\bar{q}q$ bound states. Under a chiral transformation we find [25] $U(x) \rightarrow U_L U(x) U_R^\dagger$. This is a *derived* result of the FIC analysis which is usually *assumed* in phenomenological modelling. We have included the lowest order term which depends on \mathcal{M} , i.e. for small breaking of the chiral symmetry by the quark current masses.

The coupling of the baryon states to the above mesons requires us to keep the full \mathcal{B} in analysing the baryon sector, and not just the dominant configuration value \mathcal{B}_{CQ} . However the long wavelength limit of the NG-boson-baryon coupling may be inferred from the chiral invariance of (32). Now

$$\text{TrLn} \left[(\gamma \cdot \partial + M(-\partial^2)) \delta^4(x - y) \right] = \text{TrLn} \left[(\gamma \cdot \partial + \mathcal{V}M(-\partial^2)) \delta^4(x - y) \right]$$

reflects that invariance in (32), where $\mathcal{V} = \exp(i\sqrt{2}\gamma_5\pi^a T^a)$, with $\{T^a\}$ the generators of $SU(3_f)$ **8** representation.

3.5 Hadronic Laws

Gathering the above results and keeping only the low orders in the hadronic variables and in the derivatives (appropriate to a low-energy long-wavelength expansion)

$$Z = \int D\pi D\rho D\omega \dots D\bar{N} DN \dots \exp(-S_{had}[\pi, \rho, \omega, \dots, \bar{N}, N, \dots]), \quad (38)$$

$$\begin{aligned} S_{had} [\pi, \rho, \omega, \dots, \bar{N}, N, \dots] = \\ \int d^4x \text{tr} \{ \bar{N} (\gamma \cdot \partial + M_0 + \Delta M_0 - M_0 \sqrt{2}i\gamma_5\pi^a \mathcal{T}^a + \dots) N \} \end{aligned}$$

$$\begin{aligned}
& + \int d^4x \left[\frac{f_\pi^2}{2} [(\partial_\mu \pi)^2 + m_\pi^2 \pi^2] + \frac{f_\rho^2}{2} [-\rho_\mu (-\partial^2) \rho_\mu + (\partial_\mu \rho_\mu)^2 + m_\rho^2 \rho_\mu^2] \right. \\
& + \frac{f_\omega^2}{2} [\rho \rightarrow \omega] - f_\rho f_\pi^2 g_{\rho\pi\pi} \rho_\mu \cdot \pi \times \partial_\mu \pi - i f_\omega f_\pi^3 \epsilon_{\mu\nu\sigma\tau} \omega_\mu \partial_\nu \pi \cdot \partial_\sigma \pi \times \partial_\tau \pi \\
& - i f_\omega f_\rho f_\pi G_{\omega\rho\pi} \epsilon_{\mu\nu\sigma\tau} \omega_\mu \partial_\nu \rho_\sigma \cdot \partial_\tau \pi \\
& \left. + \frac{\lambda i}{80\pi^2} \epsilon_{\mu\nu\sigma\tau} \text{tr}(\pi \cdot F \partial_\mu \pi \cdot F \partial_\nu \pi \cdot F \partial_\sigma \pi \cdot F \partial_\tau \pi \cdot F) + \dots \right], \tag{39}
\end{aligned}$$

in which the baryon octet is finally written as a rank-2 tensor, $N = N^a \mathcal{T}^a$, where the $\{\mathcal{T}^a\}$ are generators of the $SU(3_f)$ **3** representation. We have written $\lambda_j(P^2) = (P^2 + m_j(P^2)^2) f_j^2$ where $m_j(P^2)$ are the running meson masses, but only the physical masses (from $\lambda(P^2) = 0$) are shown above. The imaginary terms in this meson action are the chiral anomalies of QCD, including in particular the Wess-Zumino term. In (39) we have shown m_π and ΔM_0 which are mass terms from the chiral symmetry breaking quark current masses, while M_0 is the ‘chiral mass’ of the constituent baryons (see sect.8). For non-zero quark current masses the NG boson masses $\{m_\pi\}$ and the baryon octet mass splittings $\{\Delta m_0\}$ are seen to satisfy the Gell-Mann-Okubo and Coleman-Glashow formulae [27].

In general the coupling terms in the hadronic action are non-local and the actions in (37) and (39) will also contain higher order derivative terms like $\text{tr}\{\bar{N}(m_N \sqrt{2i\gamma_5} \partial^2 \pi^a \mathcal{T}^a + \dots) N\}$. These should not be thought of as ‘different’ couplings, but rather as just arising from the expansion of the meson-baryon vertex function $\Gamma_0(p, q)$. Hence rather than making this effective action non-renormalisable, as often occurs in effective actions, such terms when properly retained as parts of complete vertex functions actually render loop diagrams finite (an example is the pion-nucleon loop in sect.9).

The full non-local meson sector of (39) [24] has been used in many studies, such as the $\rho \rightarrow \pi\pi$ decay [23], $\omega - \rho$ mass splitting [28], charge symmetry breaking via $\rho - \omega$ mixing [29], pion loop contribution to $\rho - \omega$ mixing [30] and pion and ρ meson observables [31], for extensions to include electromagnetic interactions [32, 33], and for η and η' [36]. For the pion loop contribution to the electromagnetic pion charge radius see [34]. The chirally invariant form of the NG boson sector in (37) in particular has been investigated in [35] and the $\pi - \pi$ scattering lengths in [26].

4 Effective Gluon Correlator

We now consider the detailed implementation of the GCM. First we must determine the effective gluon correlator by fitting GCM observables to experimental data. This involves the determination of the dominant configuration, i.e. the constituent quark effect. This effective gluon correlator and quark correlator are then used in the constituent-meson BSE equations in order to determine meson masses, and also f_π . The dominant configuration is defined by equations,

$$\frac{\delta S}{\delta \mathcal{B}(x, y)}|_{\mathcal{B}_{CQ}} = 0. \tag{40}$$

Of the set $\mathcal{B}_{CQ}(x, y)$ only $A(x - y)$ and $B(x - y)$ (their Fourier transforms appear in (42)) are non-zero bilocal fields characterising the dominant configuration. They are also translation-invariant. This is the dynamical breaking of chiral symmetry. Such non-zero dominant configurations are also known as condensates. Writing out the translation invariant CQ equations we find that the dominant configuration is indeed simply the constituent quark effect as they may be written in the form of (33) or (34), or

$$G^{-1}(p) = i\rho + m + \frac{4}{3} \int \frac{d^4q}{(2\pi)^4} D_{\mu\nu}(p - q) \gamma_\mu G(q) \gamma_\nu, \tag{41}$$

which is the gluon dressing of a constituent quark. Its solution has the structure

$$G(q) = (iA(q^2; m)q.\gamma + B(q^2; m) + m)^{-1} = -iq.\gamma\sigma_v(q^2; m) + \sigma_s(q^2; m). \quad (42)$$

In the chiral limit there are more \mathcal{B}_{CQ} fields that are non-zero, and the resultant degeneracy of the dominant configuration is responsible for the masslessness of the pion. The constituent quark correlator G should not be confused with the complete quark correlator \mathcal{G} from (2) which would be needed to analyse the existence or otherwise of free quarks. The G on the other hand relates exclusively to the internal structure of hadrons, and to the fact that this structure appears to be dominated by the constituent quark effect. The evaluation of \mathcal{G} is a very difficult task, even within the GCM, while G is reasonably easy to study using (41). The truncation of the DSE in which the full quark \mathcal{G} is approximated by this G amounts to using a mean field approximation (see (53)); however from the tDSE there is no systematic formalism for going beyond the mean field as there is in the GCM. The hadronic effective action in (32) arises when $S[\mathcal{B}, \dots]$ is expanded about the dominant CQ configuration; the first derivative is zero by (40), and the second derivatives, or curvatures, give the constituent or core meson correlators $G_m(q, p; P)$

$$G_m^{-1}(q, p; P) = F.T. \left(\frac{\delta^2 S}{\delta \mathcal{B}(x, y) \delta \mathcal{B}(u, v)} \Big|_{\mathcal{B}_{CQ}} \right), \quad (43)$$

after exploiting translation invariance and Fourier transforming. Higher order derivatives lead to couplings between the meson cores. The $G_m(q, p; P)$ are given by ladder-type correlator equations and the non-ladder effects are inserted by the final functional integrals in (10), giving the complete GCM meson correlators $\mathcal{G}_m(q, p; P)$. It is interesting to note that the truncated and modified DSE in Maris and Roberts[37] are identical to (41) and (43), in the form of (44).

In the fitting to meson data the ω and a_1 mesons are described by these constituent meson correlators; that is, we ignore meson dressings of these mesons. The mass M of these states is determined by finding the pole position of $G_m(q, p; P)$ in the meson momentum $P^2 = -M^2$ and this, or equivalently the meson version of (20) which for the mass-shell has $\lambda(P^2) = 0$, leads to the homogeneous vertex equation

$$\Gamma(p; P) = -\frac{4}{3} \int \frac{d^4 q}{(2\pi)^4} D_{\mu\nu}(q - p) \gamma_\mu G(q + \frac{P}{2}) \Gamma(q; P) G(q - \frac{P}{2}) \gamma_\nu. \quad (44)$$

To solve (41) for various $D_{\mu\nu}(p)$ and then to proceed to use $A(s)$ and $B(s)$ in meson correlator equations for fitting observables to meson data is particularly difficult. A robust numerical technique is to use a separable expansion[8] as follows. We have in the Landau gauge

$$D_{\mu\nu}(p) = (\delta_{\mu\nu} - \frac{p_\mu p_\nu}{p^2}) D(p^2), \quad \text{and} \quad \mathcal{G}_{\mu\nu}(p) = (\delta_{\mu\nu} - \frac{p_\mu p_\nu}{p^2}) \mathcal{G}(p^2), \quad (45)$$

where $D(p^2) = g(p^2) \mathcal{G}(p^2) g(p^2)$. First expand $D(p - q)$ in (41) into $O(4)$ hyperspherical harmonics $D(p - q) = D_0(p^2, q^2) + q.p D_1(p^2, q^2) + \dots$, (46)

$$D_0(p^2, q^2) = \frac{2}{\pi} \int_0^\pi d\beta \sin^2 \beta D(p^2 + q^2 - 2pq \cos \beta, \dots) \quad (47)$$

Introduce a multi-rank separable D_0 expansion (here $n = 3$)

$$D_0(p^2, q^2) = \sum_{i=1,n} \Gamma_i(p^2) \Gamma_i(q^2), \quad (48)$$

and the constituent quark equations then have solutions of the form (in the chiral limit)

$$B(s) = \sum_{i=1,n} B_i(s), \quad B_i(s) = b_i \Gamma_i(s), \quad \sigma_s(s) = \sum_{i=1,n} \sigma_s(s)_i, \quad (49)$$

$$b_i^2 = 4\pi^2 \int_0^\infty s ds B_i(s) \sigma_s(s), \quad \text{and} \quad B_i(s) = \frac{\sigma_s(s)_i}{s\sigma_v(s)^2 + \sigma_s(s)^2}. \quad (50)$$

However rather than specifying Γ_i in (48) we proceed by parametrising forms for the σ_{si} and σ_v ; the Γ_i then follow from (49) and (50):

$$\begin{aligned} \sigma_s(s)_1 &= c_1 \exp(-d_1 s), \quad \sigma_s(s)_2 = c_2 \cdot \left(\frac{2s^2 - d_2(1 - \exp(-2s^2/d_2))}{2s^4} \right)^2, \\ \sigma_s(s)_3 &= c_3 \left(\frac{2f(s) - d_3(1 - \exp(-2f(s)/d_3))}{2f(s)^2} \right)^2, \quad f(s) = s(\ln(\tau + s/\Lambda^2))^{1/2} \\ \sigma_v(s) &= \frac{2s - \beta^2(1 - \exp(-2s/\beta^2))}{2s^2}. \end{aligned} \quad (51)$$

The three σ_{si} terms mainly determine the IR, midrange and UV regions; the $\sigma_s(s)_3$ term describes the asymptotic form of $\sigma_s(s) \sim 1/s^2 \ln(s/\Lambda^2)$ for $s \rightarrow \infty$ and ensures the form for $D(s) \sim 1/s \ln(s/\Lambda^2)$. The parameter $\tau = 10$ ensures that σ_3 is well behaved at small s , but otherwise has no effect on the fit. With these parametrised forms we can numerically relate, in a robust and stable manner, the parameter set in Table 1 to the mass of the $a_1(1230\text{MeV})$ and $\omega(783\text{MeV})$ mesons from (44), to $f_\pi(93.3\text{MeV})$ and to experimental $\alpha(s)$ points (see insert in Fig.7) from the Particle Properties Data Booklet for $s > 3\text{GeV}^2$.

The translation invariant form for the effective gluon correlator is easily reconstructed by using $D(p^2) = D_0(p^2, 0)$ in (46) and then from (48)

$$D(p^2) = \sum_i \frac{1}{b_i^2} \frac{\sigma_s(0)_i}{\sigma_s(0)^2} \frac{\sigma_s(p^2)_i}{p^2 \sigma_v(p^2)^2 + \sigma_s(p^2)^2}. \quad (52)$$

With the parameter set in Table 1 the resulting quark-quark coupling correlator $D(p^2)$ is shown in Fig.7 and Fig.8. A significant feature of QCD is that the infrared dominance, as revealed by the large value of $D(s)$ at small s , causes the CQ equations to saturate, i.e. the forms of the solutions $A(s)$ and $B(s)$ at low s are independent of the detailed IR form of $D(s)$. This saturation effect means that low energy QCD is surprisingly easy to model, and this effect is utilised in the GCM.

In Fig.8 we plot the new GCM98 quark-quark coupling correlator $D(s)$ which shows excellent overall agreement with the Jain-Munczek $D(s)$ [38, 39], and we also plot $D(s) = g(s)\mathcal{G}(s)g(s)$ constructed from the Marenzoni *et al.* [41] $\mathcal{G}(s)$ and Skulander [42] $g(s)$ lattice results which shows agreement down to $s = 1.8\text{GeV}^2$. The normalisation and shape of the Marenzoni *et al.* $\mathcal{G}(s)$ agrees with that of Leinweber *et al.* [40]. However the normalisation of the much more difficult lattice computation of $g(s)$ is uncertain and we have chosen it so that the combined lattice $D(s)$ agrees with the experimental Particle Properties Data Booklet for $s > 3\text{GeV}^2$. As shown in Fig.8 all three $D(s)$ depart from the two-loop form below $s = 2.5\text{GeV}^2$. The difference between the GCM98 (or Jain-Munczek) and the lattice construction could be an indication of contributions to the quark-quark coupling from higher order gluon self-couplings at low energy, since processes like Fig.3(c) would be included in the GCM fit, but are not in the lattice construction. The earlier GCM95 and GCM97 gave $D(s)$ that differed mainly in the asymptotic region, see plots in [10].

The insert in Fig.8 shows the $g(s)$ from $g^2(s) = D(s)/\mathcal{G}(s)$ that then follows from our analysis. This is the effective quark-gluon coupling vertex if the gluon correlator is taken to be that of Marenzoni *et al.* (or Leinweber *et al.*) and here the error bars now indicate combined errors and uncertainties from the lattice spacing. Also shown is $g(s)$ from Skulander[42] with the normalisation as discussed above.

We summarise in Table 2 some of the hadronic observables that may be computed within the GCM, showing in particular their sensitivity to the evolving modelling of the effective gluon correlator. Further meson observables are reviewed in Tandy [7].

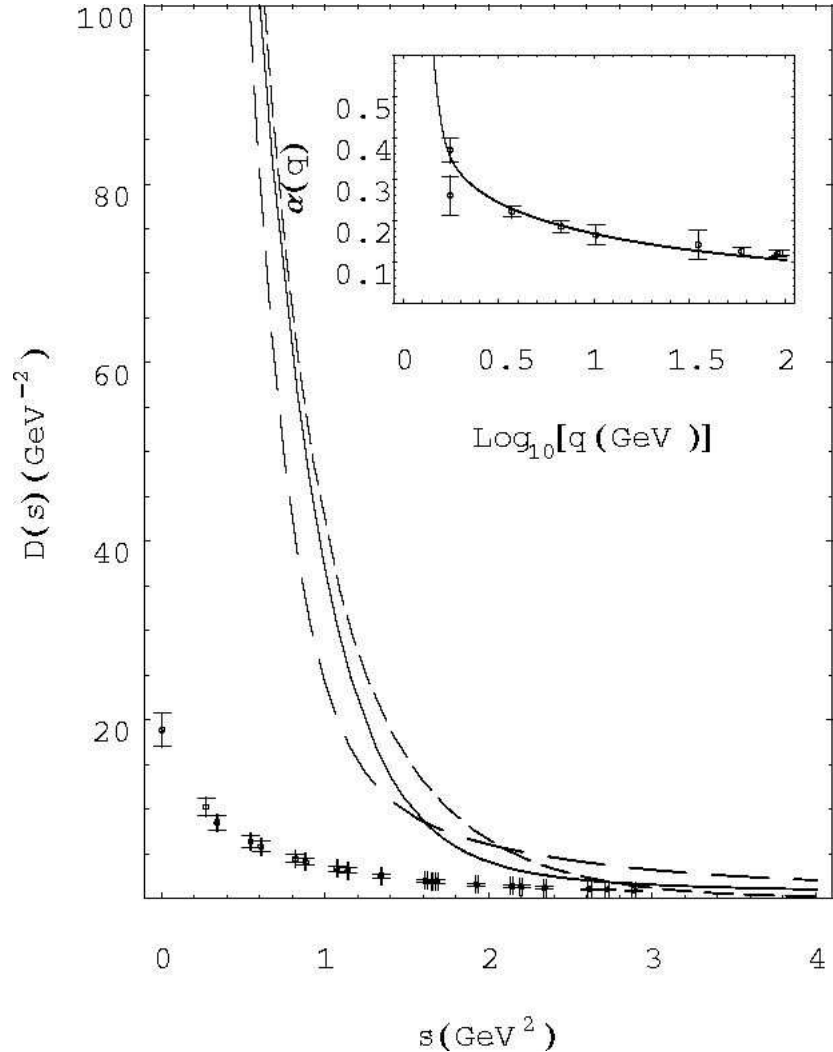


Figure 7: Plots of $D(s)$ (GeV^{-2}). Solid line is GCM98; shortdash line is GCM95; longdash line is GCM97. Data plot is lattice pure-gluon $\mathcal{G}(s)$ from Marenzoni *et al.*, and so has no quark-gluon vertex. Insert is fit of GCM98 to $\alpha(s)$ of Particle Data Book.

Table 1: GCM1998 $\sigma_s(s)$ and $\sigma_v(s)$ Parameters.

c_1	1.839GeV^{-1}	d_1	3.620GeV^{-2}	β	0.4956GeV
c_2	0.0281GeV^7	d_2	1.516GeV^4	Λ	0.234GeV
c_3	0.0565GeV^3	d_3	0.7911GeV^2		

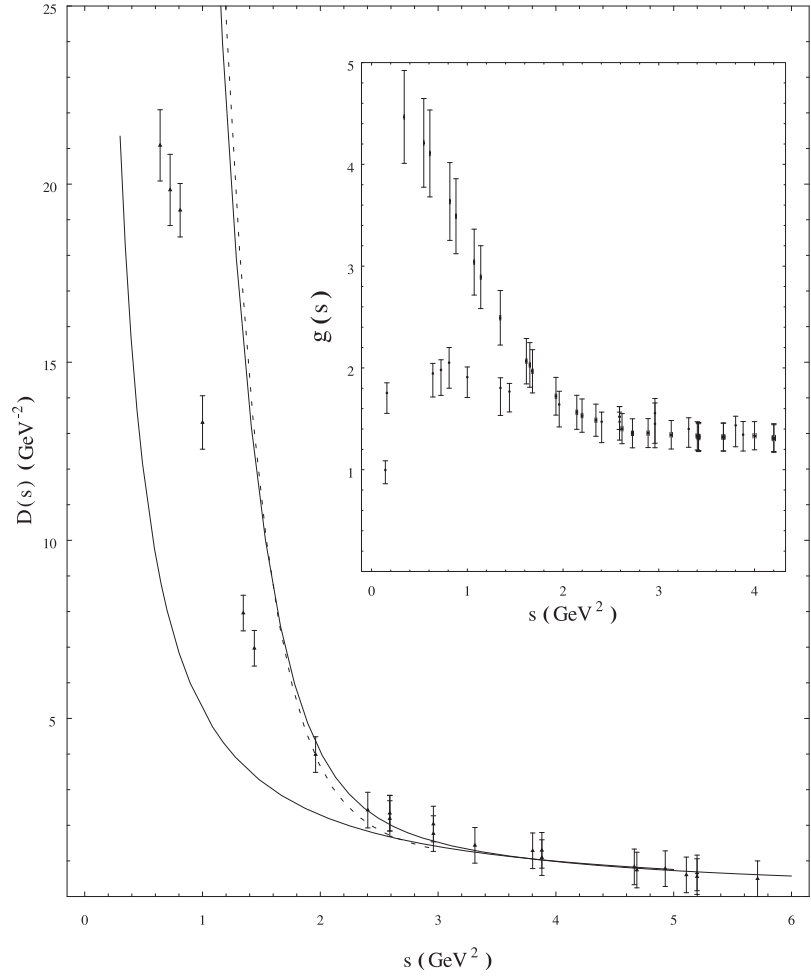


Figure 8: Plots of $D(s)$ (GeV^{-2}). GCM98 is the upper solid line which is almost identical to the Jain and Munczek $D(s)$ (dashed line); lower solid line is two-loop form with $\Lambda = 0.234\text{GeV}$, $N_f = 3$ and $\tau = 10$; data plot is combined lattice data for $g(s)\mathcal{G}(s)g(s)$ with $\mathcal{G}(s)$ from Marenzoni *et al.* (as in (a)) and $g(s)$ from Skulderud. Insert shows $g(s)$ from Skulderud (lower data plot), and from GCM98/ $\mathcal{G}(s)$ (upper data plot).

Table 2: Hadronic Observables.

Observable	GCM1995	GCM1997	GCM1998	Expt/Theory
f_π	93.0MeV*	93.2MeV*	92.40MeV*	93.3MeV
a_1 meson mass	1230MeV*	1231MeV*	1239MeV*	1230MeV
π meson mass(for $m_{u,d}$)	138.5MeV*	138.5MeV*	138.5MeV*	138.5MeV
$\alpha(s)$	-	-	fitted	†
K meson mass (for m_s)	496MeV*	-	-	496MeV
$(m_u + m_d)/2 _R(\mu = 1\text{GeV})$	6.5MeV	4.8MeV	7.7MeV	$\approx 8.0\text{MeV}$
$m_s _R(\mu = 1\text{GeV})$	135MeV	-	-	130MeV
ω meson mass	804MeV	783MeV*	783MeV*	782MeV
$a_0^0 \pi - \pi$ scatt. length	0.1634	0.1622	0.1657	0.26 ± 0.05
$a_0^2 \pi - \pi$ scatt. length	-0.0466	-0.0463	-0.0465	-0.028 ± 0.012
$a_1^1 \pi - \pi$ scatt. length	0.0358	0.0355	0.0357	0.038 ± 0.002
$a_2^0 \pi - \pi$ scatt.length	0.0017	0.0016	0.0018	0.0017 ± 0.003
$a_2^2 \pi - \pi$ scatt.length	-0.0005	-0.0005	-0.0003	$.00013 \pm 0.0003$
r_π pion charge radius	0.55fm	0.53fm	0.53fm	0.66fm
$\frac{1}{2}^+(0^+)$ nucleon-core mass**	1390MeV	1435MeV	1450MeV	$>1300\text{MeV}††$
const. quark rms size	0.51fm	0.39fm	0.58fm	-
chiral quark const. mass	270MeV	267MeV	325MeV	-
0^+ diquark rms size	0.55fm	0.55fm	0.59fm	-
0^+ diquark const. mass	692MeV	698MeV	673MeV	$>400\text{MeV}$
1^+ diquark const. mass	1022MeV	903MeV	933MeV	-
0^- diquark const. mass	1079MeV	1049MeV	1072MeV	-
1^- diquark const. mass	1369MeV	1340MeV	1373MeV	-
MIT bag constant	$(154\text{MeV})^4$	$(145\text{MeV})^4$	$(166\text{MeV})^4$	$(146\text{MeV})^4$
MIT N-core (no cms corr.)	1500MeV	1420MeV	1625MeV	$>1300\text{MeV}††$

* fitted observable; - not computed or not known; † $\alpha(s)$ from Particle Properties Data Booklet; GCM1995: [8]; GCM1997: [9]; GCM1998: [10].
** only 0^+ diquark correlation; 1^+ diquark correlation lowers nucleon core mass.
†† nucleon core mass (i.e. no meson dressing).

5 Constituent Quarks

The constituent quark effect [43] is the dominant effect in determining the structure of hadrons, and also their response in scattering events, particularly deep inelastic scattering. The constituent mass effect manifested itself in the early studies of baryon magnetic moments. The GCM analysis reveals rather directly both the effective mass and the effective size of the constituent quarks, and relates these to the effective gluon correlator. We consider chiral limit constituent quarks and we carefully define constituent quarks and constituent hadrons as those constructs appearing in exponentiated effective actions in the functional formulation of the GCM and distinguish them from the exact correlations, which follow from the complete functional integrations. We can express the full quark correlator $\mathcal{G}(x, y)$ in terms of the bosonised FIC variables, with (2) and (17) giving

$$\mathcal{G}(x, y) = \frac{\int D\mathcal{B} D\mathcal{D} D\mathcal{D}^* G(x, y, \mathcal{B}) \exp(-S[\mathcal{B}, \mathcal{D}, \mathcal{D}^*])}{\int D\mathcal{B} D\mathcal{D} D\mathcal{D}^* \exp(-S[\mathcal{B}, \mathcal{D}, \mathcal{D}^*])}, \quad (53)$$

where $G(x, y, \mathcal{B})$ is defined in (16). The bilocal field functional integrals can be further decomposed into local hadronic functional integrals. The constituent quark effect appears as the dominant configuration about which the meson-diquark bosonised GCM action in (53) (and elsewhere) is expanded. This is characterised by $\mathcal{D} = 0$ and two of the $\mathcal{B} \neq 0$ (the \mathcal{B}_{CQ}). At the dominant configuration $G(x, y, \mathcal{B}_{CQ})$ is the constituent quark correlator which appears in the constituent

meson and baryon correlators. The \mathcal{B}_{CQ} eqns.(34) have the form (we use a Feynman-like gauge to simplify the discussion, but the more realistic Landau gauge may be used),

$$B(p^2) = \frac{16}{3} \int \frac{d^4 q}{(2\pi)^4} D(p-q) \cdot \frac{B(q^2)}{q^2 A(q^2)^2 + B(q^2)^2}, \quad (54)$$

$$[A(p^2) - 1]p^2 = \frac{8}{3} \int \frac{d^4 q}{(2\pi)^4} q \cdot p D(p-q) \cdot \frac{A(q^2)}{q^2 A(q^2)^2 + B(q^2)^2}. \quad (55)$$

Here $B(q^2)$ and $C(q^2) = A(q^2) - 1$ are the Fourier transforms of the two $\mathcal{B}_{CQ}(x, y)$ fields, and where translational invariance is used: $\mathcal{B}_{CQ}(x, y) \rightarrow \mathcal{B}_{CQ}(x - y)$. We see from (53) that the full quark correlator is given by the dressing of the constituent quark correlator by various hadronic fluctuations. In the context of the tDSE (54) and (55) (in Landau gauge) are often used as an approximation [37] to the full quark correlator; $\mathcal{G}(x, y) \approx G(x, y, \mathcal{B}_{CQ})$, thereby confusing the full and constituent quark correlators. The GCM formulation clearly reveals that the tDSE approach is actually using a mean field approximation. The additional processes manifest in (53) show up in the FIC hadronisation as the dressing of constituent hadrons by other hadrons, of which the pion dressing of the nucleon is the most pronounced example. These dressings incorporate additional processes corresponding to further dressing of the constituent quarks as well as further interactions between the constituent quarks.

When considering only the constituent quarks the bilocal effective action in (53) may be simplified by keeping only the translation invariant B and C dependence. This leads to a reduced action per quark flavour,

$$S_{CQ}[B, C] = V \left(-\frac{12\pi^2}{(2\pi)^4} \int dq q^3 \ln(A^2(q^2)q^2 + B(q^2)^2) \right. \\ \left. + \frac{9}{4}\pi^2 \int dx x^3 \frac{B(x)^2}{D(x)} + \frac{9}{2}\pi^2 \int dx x^3 \frac{C(x)^2}{D(x)} \right) \quad (56)$$

where V is the (infinite) spacetime volume. The minimization of $S_{CQ}[B, C]$ gives (54) and (55). The action $S_{CQ}[B, C]$ has the form of a sum of a *kinetic energy* term (defined as that part which is local in momentum) and a *potential energy* term (defined as that part which is local in relative spacetime). Both have unconventional forms because (56) describes self-interaction effects. The kinetic energy term involves the constituent quark running mass $M(s) = B(s)/A(s)$.

Since the key constituent quark effective mass is associated with the kinetic part of (56), we subtract the $B = 0$ form. In this way we compare the non-perturbative configuration with the perturbative configuration, and it is this difference which also generates the MIT bag constant discussed in sect.10,

$$S_{CQ}[B] = V \left(-\frac{12\pi^2}{(2\pi)^4} \int_0^{+\infty} dq \left[q^3 \ln \left(\frac{A(q^2)^2 q^2 + B(q^2)^2}{A^2(q^2)q^2} \right) \right] + \frac{9}{4}\pi^2 \int_0^{+\infty} dx \left[x^3 \frac{B(x)^2}{D(x)} \right] \right). \quad (57)$$

The kinetic energy and potential energy integrands, indicated by the square brackets in (57), are shown in Fig.9. Fig.9(a) also shows the quark running mass. The chiral limit constituent quark mass of approximately 300MeV is revealed as the value of the running mass that dominates the kinetic energy integrations. The width of the q -integrations being a ‘fermi-motion’ effect. The integrand of the potential energy term shows that gluon exchanges up to some 1.2fm are relevant. Hence we see directly that the constituent quark characteristics are implicit in the action (56).

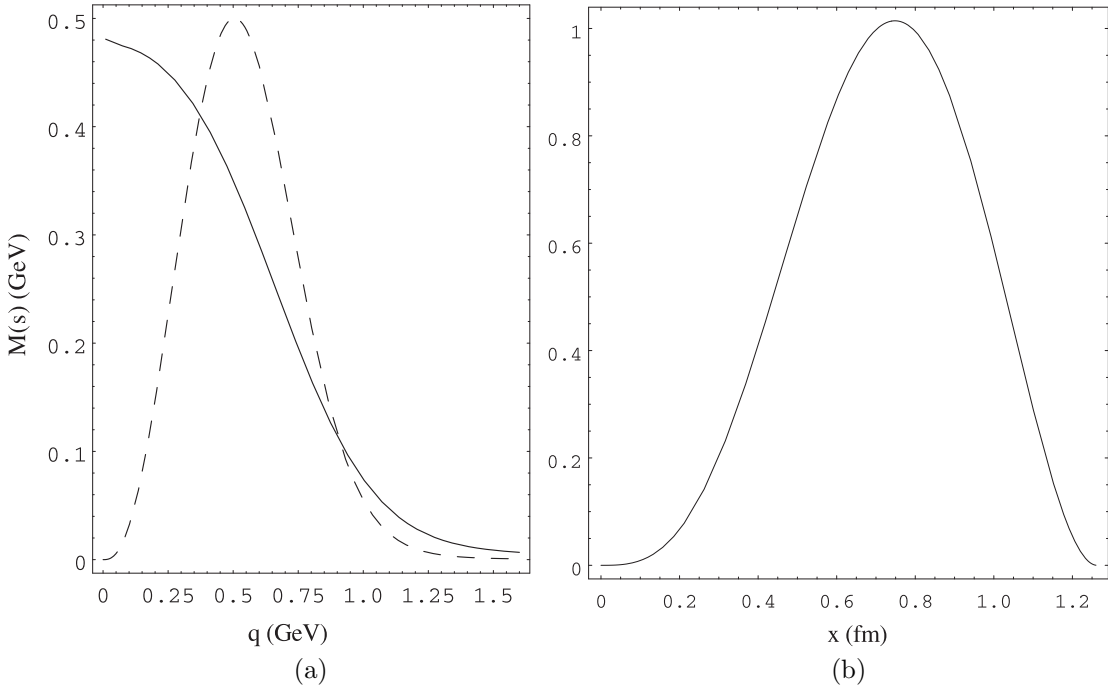


Figure 9: (a) Quark running mass $M(s)$ (solid line) and the integrand of the kinetic energy part of the constituent quark action. (b) Integrand of the potential energy part of the constituent quark action.

6 Constituent Mesons and Diquarks

From the hadronisation we saw that the constituent mesons and diquarks arise as ladder BSE states; with their correlators described as the generalised curvatures of the meson-diquark boson action when expanding about the dominant or constituent quark configuration. This provides a particularly instructive insight into the true role of such ladder BSE states. Traditionally these ladder states arose as a severe truncation of the full coupled DSE, however we see that they actually play a key dynamical role in the hadronisation in that they naturally arise as appropriate FIC variables, rather than from some unstructured approximation scheme. The crossed diagrams that are normally neglected in the tDSE are automatically inserted in the GCM via the hadronic functional integrations in (38), and it is these processes that convert the constituent mesons and baryons into the observable hadronic modes, as seen later in sect.9 for the nucleon. Hence the GCM hadronisation reveals a ‘book-keeping’ that was not previously known. In this connection Bender, Roberts and von-Smeckal [22] have found evidence that these additional crossed gluon processes may be responsible for confining the diquarks, which is particularly interesting since the ladder BSE have a mass-shell for the diquarks, and it is these masses which are shown in Table 2, see also [44]. That study explicitly included the crossed diagrams by extending the BSE equation to include the lowest order crossed diagram. However in the GCM hadronisation such crossed diagrams are seen to arise from meson exchanges, as shown in Fig.10. Evidence from the nucleon computations suggests that due to the high ‘constituent mass’ of the diquarks the presence of the pole in the diquark correlator at the mass-shell is not dynamically significant.

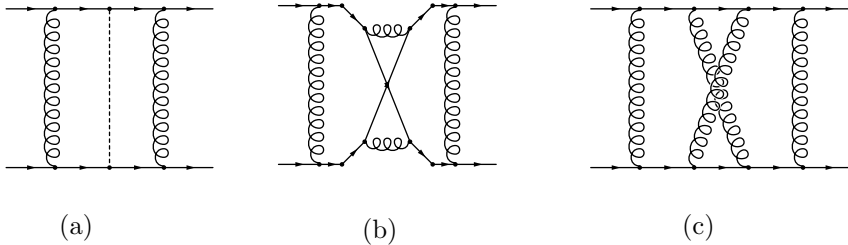


Figure 10: (a) Diagram shows a meson exchange from the functional integral in (56), dressing constituent ladder diquark correlations. (b) a low order gluon process within the meson exchange. In (c) we redraw (b) to show the crossed gluon processes inserted via meson exchange.

The connection between the bilocal meson-diquark action and the ladder BSE states inspired an insightful alternative to the solving of the linear homogeneous BSE. This analysis in Cahill, Roberts and Praschifka [45] involved re-formulating the ladder BSE, in which the boson mass of interest M occurs implicitly in the quark correlators, as an explicit mass functional. As an example, for the scalar diquark state 0^+ we find

$$M[\Gamma]^2 = -\frac{24}{f[\Gamma]^2} \int \frac{d^4 q}{(2\pi)^4} \frac{\Gamma(q)^2}{A(q)^2 q^2 + B(q)^2} + \frac{9}{f[\Gamma]^2} \int d^4 x \frac{\Gamma(x)^2}{D(x)}, \quad (58)$$

where $f[\Gamma]$ is a normalisation functional [45]. The minimisation of $M[\Gamma]$ with respect to the boson vertex function Γ then yields the mass $M > 0$, at least as a good approximation for the low mass mesons and diquarks. A similar expression for the pion mass functional $M_\pi[\Gamma]$ is given by (58), but with $9 \rightarrow 9/2$ in the second term (the Landau gauge version, in the near chiral limit, is given in (73)). Then the minimum of $M_\pi[\Gamma] = m_\pi = 0$ arises for $\Gamma(q) = B(q)$, as follows from the minimisation of $S_{CQ}[B]$ in (57). However another feature of the GCM comes into play when we use the property that all the low mass mesons and diquarks have approximately the same $\Gamma(q)$, and that this is merely the $B(q)$ function of the constituent quark correlator (an exact result for the pion). This intricate relationship is again a consequence of the dominance of the constituent quark effect. Hence using $\Gamma = B$ in (58) then yields an explicit value for the constituent mass of the 0^+ diquark. Similar mass functionals for the other states are given in [45].

7 Constituent Nambu-Goldstone Mesons

The properties of the pion continue to be the subject of considerable theoretical and experimental interest in QCD studies. The pion is an (almost) massless NG boson and its properties are directly associated with dynamical chiral symmetry breaking and the underlying quark-gluon dynamics. The GCM is particularly effective in revealing the NG phenomena that follows from the dynamical breaking of chiral symmetry [25, 26]. Indeed the GCM results in the complete derivation of the Chiral Perturbation Theory (ChPT) phenomenology, but with the added feature that again the induced NG effective action is non-local, so that the usual non-renormalisability problems do not arise (see sect.3.4). However again we must distinguish the full NG degrees of freedom from the constituent NG modes, as again this distinction is often missing, particularly in the tDSE formulation. The full NG (pion) correlator \mathcal{G}_π is the connected part of

$$\mathcal{G}_\pi(x, y, z, w) = \int D\bar{q} Dq D\bar{q}(x) i\gamma_5 \tau_i q(y) \bar{q}(z) i\gamma_5 \tau_i q(w) \exp(-S_{GCM}[A, \bar{q}, q]) \quad (59)$$

or, from the hadronisation (10),

$$\mathcal{G}_\pi(X, Y) = \int D\pi.. D\bar{N} D\bar{N}.. \pi(X) \pi(Y) \exp(-S_{had}[\pi, \dots, \bar{N}, N, \dots]) \quad (60)$$

in which $X = \frac{x+y}{2}$ and $Y = \frac{z+w}{2}$ are ‘centre-of-mass’ coordinates for the pion. We note that now the pion field appears in $S_{had}[\pi, \dots, \bar{N}, N, \dots]$ in the exponent of (60), with an effective-action mass parameter m_π ; see (39). It is important to clearly distinguish this mass, together with the equations which define its value, from the pion mass that would emerge from the evaluation of the functional integrals in (59) or (60). Equation (59) or (60) defines the observable pion mass, whereas the mass in the exponent defines the constituent pion mass. There is no reason for these to be equal in magnitude, though they may well both be given by the generic Gell-Mann-Oakes-Renner (GMOR)[46] formula.

$$m_\pi^2 = \frac{12}{f_\pi^2} \int \frac{d^4 q}{(2\pi)^4} (m_u(s) + m_d(s)) \sigma_s(q^2) + O(m^2). \quad (61)$$

Recently there has been a derivation[47, 48, 49] of an alternative mass formula and the demonstration of its equivalence to the GMOR formula for the constituent pion mass, which we briefly consider. That derivation exploited the intricate interplay between the constituent pion Bethe-Salpeter equation (BSE) and the non-linear CQ equation, resulting in the new expression

$$m_\pi^2 = \frac{48m}{f_\pi^2} \int \frac{d^4 q}{(2\pi)^4} (\epsilon_s(s) \sigma_s(s) + s \epsilon_v(s) \sigma_v(s)) c(s) + O(m^2), \quad (62)$$

where $c(s)$ is the function

$$c(s) = \frac{B(s)^2}{sA(s)^2 + B(s)^2}, \quad (63)$$

where $A(s)$ and $B(s)$ are the chiral limit of $A(s; m)$ and $B(s; m)$, and where $\epsilon_s(s)$ and $\epsilon_v(s)$ are functions which specify the response of the constituent quark correlator to the turning on of the quark current mass, defined, for small $m \neq 0$, by the expansions in $m(s)$

$$B(s; m) + m(s) = B(s) + m(s) \cdot \epsilon_s(s) + O(m^2), \quad (64)$$

$$A(s, m) = A(s) + m(s) \cdot \epsilon_v(s) + O(m^2). \quad (65)$$

For large space-like s we find that $\epsilon_s \rightarrow 1$, but for small s we find that $\epsilon_s(s)$ can be significantly larger than 1. This is an infrared-region dynamical enhancement of the quark current mass by gluon dressing, and indicates the strong response of the chiral limit constituent quark correlator to the turning on of the current mass. A plot of $\epsilon_s(s)$ is shown in [47]. The GCM involves the solution of CQ integral equations (41) for the constituent correlation functions. Separating this CQ into its scalar and vector parts, we obtain in Landau gauge

$$B(p^2; m) = 4 \int \frac{d^4 q}{(2\pi)^4} D(p - q) \cdot \frac{B(q^2; m) + m(s)}{q^2 A(q^2; m)^2 + (B(q^2; m) + m(s))^2}, \quad (66)$$

$$[A(p^2; m) - 1]p^2 = \frac{4}{3} \int \frac{d^4 q}{(2\pi)^4} D(p - q) \left(p \cdot q + 2 \frac{q \cdot (p - q) p \cdot (p - q)}{(p - q)^2} \right) \cdot \frac{A(q^2; m)}{q^2 A(q^2; m)^2 + (B(q^2; m) + m(s))^2}. \quad (67)$$

which are (54) and (55) (which however are in Feynman gauge) with non-zero quark current mass. We have included, for generality, a phenomenological momentum dependent current mass $m(s)$ for the quarks. The usual procedure is to introduce a cutoff Λ , and to choose an s independent $m(s)$, but with the value of that constant m now Λ dependent. This is in fact our final choice. However our analysis supports a more general result with $m(s)$ dependent on s ; then the GMOR relation in

(61) has the $m(s)$ included inside the integration. Using Fourier transforms (66) may be written in the form, here for $m = 0$,

$$D(x) = \frac{1}{4} \frac{B(x)}{\sigma_s(x)}, \quad (68)$$

which implies that knowledge of the chiral-limit constituent quark correlator determines the effective gluon correlator. Multiplying (68) by $B(x)/D(x)$, and using Parseval's identity for the RHS, we obtain the identity

$$\int d^4x \frac{B(x)^2}{D(x)} = 4 \int \frac{d^4q}{(2\pi)^4} B(q) \sigma_s(q). \quad (69)$$

The second basic equation is the ladder form BSE for the constituent pion mass-shell state, which arises from the mesonic fluctuations about the minimum determined by (66) and (67),

$$\Gamma^f(p, P) = 2 \int \frac{d^4q}{(2\pi)^4} D(p - q) \text{tr}_{SF}(G_+ T^g G_- T^f) \Gamma^g(q, P) \quad (70)$$

where $G_{\pm} = G(q \pm \frac{P}{2})$. This is (44) in Landau gauge for isovector NG bosons, and only the dominant $\Gamma = \Gamma^f T^f i\gamma_5$ amplitude is retained. The spin trace arises from projecting onto this dominant amplitude. Here $\{T^b, b = 1, \dots, N_F^2 - 1\}$ are the generators of $SU(N_F)$, with $\text{tr}(T^f T^g) = \frac{1}{2} \delta_{fg}$.

The BSE (70) is an implicit equation for the mass shell $P^2 = -m_\pi^2$. It has solutions *only* in the time-like region $P^2 \leq 0$. Fundamentally this is ensured by (66) and (67) being the specification of an absolute minimum of an effective action after a bosonisation. Nevertheless the loop momentum is kept in the space-like region $q^2 \geq 0$; this mixed metric device ensures that the quark and gluon correlators remain close to the real space-like region where they have been most thoroughly studied. Very little is known about these correlators in the time-like region $q^2 < 0$.

The non-perturbative quark-gluon dynamics are expressed here in (66) and (67). Even when $m = 0$ (66) can have non-perturbative solutions with $B \neq 0$. This is the dynamical breaking of chiral symmetry. When $m = 0$ (70) has a solution for $P^2 = 0$; the Goldstone theorem effect. For the zero linear momentum state $\{\vec{P} = \vec{0}, P_4 = 0\}$ it is easily seen that (70) reduces to (66) with $\Gamma^f(q, 0) = B(q^2)$. When $\vec{P} \neq \vec{0}$ then $\Gamma^f(q, P) \neq B(q)$, and (70) must be solved for $\Gamma^f(q, P)$.

Because the pion mass m_π is small when m is small, we can perform an expansion of the P_μ dependence in the kernel of (70). Since the analysis is Lorentz covariant we can, without loss of validity, choose to work in the rest frame with $P = (\vec{0}, im_\pi)$, giving

$$\begin{aligned} \Gamma(p) = & \frac{1}{6} m_\pi^2 \int \frac{d^4q}{(2\pi)^4} D(p - q) I(s) \Gamma(q) + \\ & + 4 \int \frac{d^4q}{(2\pi)^4} D(p - q) \frac{1}{s(A(s) + m(s).\epsilon_v(s))^2 + (B(s) + m(s).\epsilon_s(s))^2} \Gamma(q) + \dots, \end{aligned} \quad (71)$$

where

$$I(s) = 6 (\sigma_v^2 - 2(\sigma_s \sigma'_s + s \sigma_v \sigma'_v) - s(\sigma_s \sigma''_s - (\sigma'_s)^2) - s^2(\sigma_v \sigma''_v - (\sigma'_v)^2)). \quad (72)$$

By using Fourier transforms the integral equation (71), now with explicit dependence on m_π , can be expressed in the form of a variational mass functional,

$$\begin{aligned} M_\pi[\Gamma]^2 = & -\frac{24}{f_\pi[\Gamma]^2} \int \frac{d^4q}{(2\pi)^4} \frac{\Gamma(q)^2}{s(A(s) + m(s).\epsilon_v(s))^2 + (B(s) + m(s).\epsilon_s(s))^2} + \\ & + \frac{6}{f_\pi[\Gamma]^2} \int d^4x \frac{\Gamma(x)^2}{D(x)}, \end{aligned} \quad (73)$$

which is equivalent to (58) for the pion (but in the Feynman gauge), and in which

$$f_\pi[\Gamma]^2 = \int \frac{d^4q}{(2\pi)^4} I(s)\Gamma(q)^2. \quad (74)$$

The functional derivative $\delta M_\pi[\Gamma]^2/\delta\Gamma(q) = 0$ reproduces (71). The mass functional (73) and its minimisation is equivalent to the constituent pion BSE in the near chiral limit. To find an estimate for the minimum we need only note that the change in m_π^2 from its chiral limit value of zero will be of 1st order in m , while the change in $\Gamma(q)$ from its chiral limit value $B(q^2)$ will be of 2nd order in m .

Hence to obtain m_π^2 to lowest order in m , we may replace $\Gamma(q)$ by $B(q^2)$ in (73), and we have that the constituent pion mass is given by

$$\begin{aligned} m_\pi^2 = & \frac{48}{f_\pi[B]^2} \int \frac{d^4q}{(2\pi)^4} m(s) \frac{\epsilon_s(s)B(s) + s\epsilon_v(s)A(s)}{sA(s)^2 + B(s)^2} \frac{B(s)^2}{sA(s)^2 + B(s)^2} \\ & - \frac{24}{f_\pi[B]^2} \int \frac{d^4q}{(2\pi)^4} \frac{B(s)^2}{sA(s)^2 + B(s)^2} + \frac{6}{f_\pi[B]^2} \int d^4x \frac{B(x)^2}{D(x)} + O(m^2) \end{aligned} \quad (75)$$

However the pion mass has been shown to be zero in the chiral limit. This is confirmed as the two $O(m^0)$ terms in (75) cancel because of the identity (69). Note that it might appear that f_π would contribute an extra m dependence from its kernel in (72). However because the numerator in (73) is already of order m , this extra contribution must be of higher order in m .

Hence we finally arrive at the analytic expression, to $O(m)$, for the constituent NG boson (mass)² from the solution of the BSE,

$$m_\pi^2 = \frac{48}{f_\pi[B]^2} \int \frac{d^4q}{(2\pi)^4} m(s) \frac{\epsilon_s(s)B(s) + s\epsilon_v(s)A(s)}{sA(s)^2 + B(s)^2} \frac{B(s)^2}{sA(s)^2 + B(s)^2} + O(m^2). \quad (76)$$

It would appear that expression (76) is manifestly different to the conventional GMOR form in (61).

However here we generalise the identity found by Langfeld and Kettner [48] that shows these forms to be equivalent. Inserting (64) and (65) into (66), and expanding in powers of $m(s)$, we obtain up to terms linear in m , and after using (66) with $m = 0$ to eliminate the $O(m^0)$ terms,

$$\begin{aligned} m(p^2)\epsilon_s(p^2) = m(p^2) & + 4 \int \frac{d^4q}{(2\pi)^4} D(p-q) \frac{m(q^2)\epsilon_s(q^2)}{q^2 A(q^2)^2 + B(q^2)^2} \\ & - 4 \int \frac{d^4q}{(2\pi)^4} D(p-q) \frac{B(q^2)^2 2m(q^2)\epsilon_s(q^2)}{(q^2 A(q^2)^2 + B(q^2)^2)^2} \\ & - 4 \int \frac{d^4q}{(2\pi)^4} D(p-q) \frac{B(q^2)A(q^2)2m(q^2)q^2\epsilon_v(q^2)}{(q^2 A(q^2)^2 + B(q^2)^2)^2}. \end{aligned} \quad (77)$$

We now multiply (77) throughout by $B(p^2)/(p^2 A(p^2)^2 + B(p^2)^2)$, and integrate wrt p . Using again the chiral limit of (66) there is some cancellation of terms, and we are left with a generalised Langfeld-Kettner identity

$$\begin{aligned} 2 \int d^4p \frac{B(p^2)^2}{p^2 A(p^2)^2 + B(p^2)^2} \left(\frac{B(p^2)m(p^2)\epsilon_s(p^2)}{p^2 A(p^2)^2 + B(p^2)^2} + \frac{p^2 A(p^2)m(p^2)\epsilon_v(p^2)}{p^2 A(p^2)^2 + B(p^2)^2} \right) = \\ \int d^4p \frac{m(p^2)B(p^2)}{p^2 A(p^2)^2 + B(p^2)^2}. \end{aligned} \quad (78)$$

Remarkably we see on using this identity that (76) is identical to (61).

8 Constituent Nucleon

We report here progress in calculating the constituent nucleon which emerges from the GCM hadronisation as a three constituent-quark state, bound by the effective gluon correlator. This nucleon state is treated as a correlation between a constituent quark and a constituent diquark subcorrelation in the separable Faddeev approach. The first such computation was in 1989 [50] and used a rank-1 description of the scalar diquark; this yielded a constituent core mass of approximately 1.3GeV, which was very close to the expected core mass [51]. A full calculation of the nucleon core mass is particularly difficult and has yet to be attempted, as it requires the inclusion of the constituent quark correlators and the various constituent diquark correlators, but particularly that of the scalar 0^+ and vector 1^+ diquarks. This nucleon core state then has its mass further reduced by pion dressing. As preparation for these extensive *ab initio* computations we have been monitoring the response of the nucleon core to the underlying low energy quark-gluon processes by computing the quark - scalar-diquark nucleon core state. The results are shown for GCM95 (rank 2), GCM97 (rank 3) and GCM98 (rank 3) in Table 2. We now briefly outline the present procedures used in these studies. Working in a Euclidean metric the equation for the spin $\frac{1}{2}^+$ nucleon form factor separable components (each a spinor) is

$$\Psi_i(p; P) = \frac{1}{6} \sum_{jk} \int \frac{d^4 q}{(2\pi)^4} \Gamma_i((p + \frac{1}{2}q + \frac{2-3\alpha}{2}P)^2) \Gamma_j((q + \frac{1}{2}p + \frac{2-3\alpha}{2}P)^2) \\ .G((2\alpha-1)P - p - q)G((1-\alpha)P + q)Z_{jk}((\alpha P - q)^2)\Psi_k(q; P), \quad (79)$$

where the Ψ_k are defined in terms of an arbitrary momentum partitioning parameter α . Here the scalar diquark correlator is modelled using the separable form

$$\Delta(q, p, P) = \sum_{ij} \Gamma_i(q) Z_{ij}(P) \Gamma_j(p), \quad (80)$$

where q and p are the relative quark momenta, and P is the diquark momentum. The matrix Z_{ij} is determined from the diquark version of the ladder BS correlator (43) when the gluon correlator separable expansion (48) is used, and only the $O(4)$ invariant part is retained. This diquark separable expansion is not to be confused with the formal expansion in (21). This nucleon core equation requires careful determination of its only ingredients, the quark correlator and the diquark correlator, and particularly its vertex functions. These are determined by solving the diquark BSE using the separable representation of the effective gluon correlator. No integration cutoffs are required.

We seek solutions to (79) (which being a homogeneous linear equation will only have solutions for particular $P^2 = -M_0^2$) which give the nucleon core mass. We work in the rest frame of the nucleon and accordingly set $P = (\mathbf{0}, iM_0)$. With the above choices of Γ , G , Z and P , (79) enjoys a spatial $O(3)$ symmetry. A direct calculation shows that the integral operator commutes with the angular momentum operator $\mathbf{J} = \mathbf{L} + \mathbf{S} = i\frac{\partial}{\partial \mathbf{p}} \times \mathbf{p} + \frac{1}{2}\boldsymbol{\sigma}$, so we take the Ψ_k to be one of the general $L = 0$, $S = \frac{1}{2}^+$ states

$$\Psi_{\uparrow k} = \begin{pmatrix} \begin{pmatrix} 1 \\ 0 \end{pmatrix} u_k(p) \\ \frac{\boldsymbol{\sigma} \cdot \mathbf{p}}{|\mathbf{p}|} \begin{pmatrix} 1 \\ 0 \end{pmatrix} v_k(p) \end{pmatrix} \quad \text{or} \quad \Psi_{\downarrow k} = \begin{pmatrix} \begin{pmatrix} 0 \\ 1 \end{pmatrix} u_k(p) \\ \frac{\boldsymbol{\sigma} \cdot \mathbf{p}}{|\mathbf{p}|} \begin{pmatrix} 0 \\ 1 \end{pmatrix} v_k(p) \end{pmatrix}, \quad (81)$$

where u_k and v_k are functions only of p_4 and $|\mathbf{p}|$. Equation (79) then becomes

$$\begin{pmatrix} u_i(p) \\ v_i(p) \end{pmatrix} = \sum_k \int \frac{d^4 q}{(2\pi)^4} K_{ik}(p_4, |\mathbf{p}|; q_4, |\mathbf{q}|; \mathbf{p} \cdot \mathbf{q}) \begin{pmatrix} u_k(q) \\ v_k(q) \end{pmatrix}, \quad (82)$$

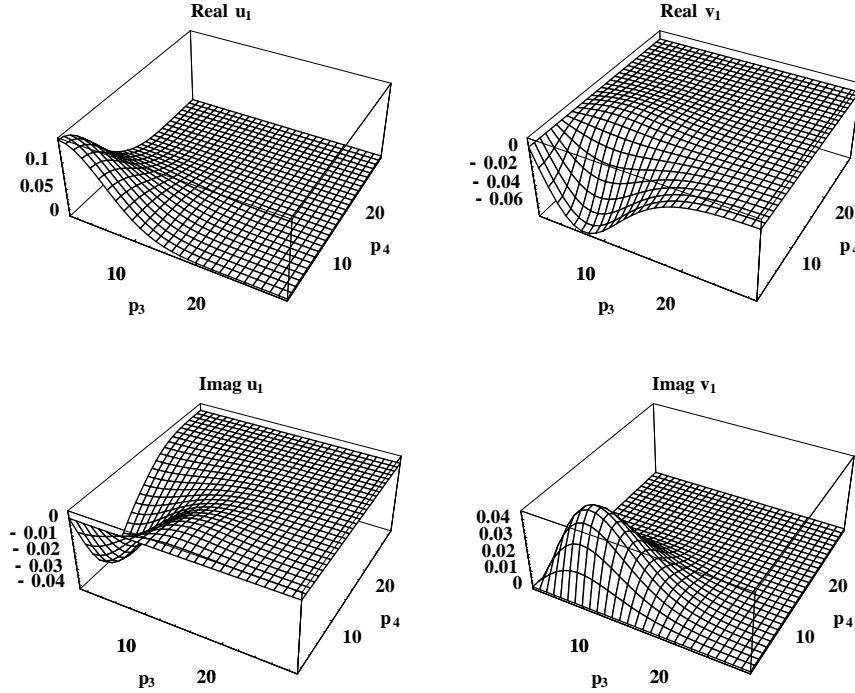


Figure 11: The real and imaginary parts of the $u_1(p_3, p_4)$ and $v_1(p_3, p_4)$ components (corresponding to the Γ_1 in (80)) of the nucleon wave function (scale: 10 units $\equiv 0.57$ GeV.)

$$K_{ik}(p_4, |\mathbf{p}|; \mathbf{q}_4, |\mathbf{q}|; \mathbf{p} \cdot \mathbf{q}) = \frac{1}{6} \sum_j \Gamma_i \left((p_4 + \frac{1}{2}q_4 + \frac{2-3\alpha}{2}iM_0)^2 + |\mathbf{p} + \frac{1}{2}\mathbf{q}|^2 \right) \cdot \Gamma_j(p \leftrightarrow q) \tilde{G}_1 \tilde{G}_2 Z_{jk}(s_3),$$

$$\tilde{G}_1 = \frac{1}{s_1 A^2(s_1) + B^2(s_1)} \begin{pmatrix} ((2\alpha-1)M_0 + i(p_4+q_4))A(s_1) + B(s_1) & (|\mathbf{q}| + \frac{\mathbf{p} \cdot \mathbf{q}}{|\mathbf{q}|})A(s_1) \\ (|\mathbf{p}| + \frac{\mathbf{p} \cdot \mathbf{q}}{|\mathbf{p}|})A(s_1) & (\tilde{G}_1)_{22} \end{pmatrix},$$

$$\text{where } (\tilde{G}_1)_{22} = [-((2\alpha-1)M_0 + i(p_4+q_4))A(s_1) + B(s_1)] \frac{\mathbf{p} \cdot \mathbf{q}}{|\mathbf{q}| |\mathbf{p}|},$$

$$\tilde{G}_2 = \frac{1}{s_2 A^2(s_2) + B^2(s_2)} \begin{pmatrix} ((1-\alpha)M_0 - iq_4)A(s_2) + B(s_2) & -|\mathbf{q}| A(s_2) \\ |\mathbf{q}| A(s_2) & -((1-\alpha)M_0 - iq_4)A(s_2) + B(s_2) \end{pmatrix},$$

and the arguments of the quark and diquark correlators are

$$\left. \begin{aligned} s_1 &= (p_4 + q_4 - (2\alpha - 1)iM_0)^2 + |\mathbf{p} + \mathbf{q}|^2, \\ s_2 &= (q_4 + (1 - \alpha)iM_0)^2 + |\mathbf{q}|^2, \\ s_3 &= (q_4 - i\alpha M_0)^2 + |\mathbf{q}|^2. \end{aligned} \right\} \quad (83)$$

Equation (82) reduces to n (the rank of the gluon correlator modelling) coupled two-dimensional integral equations after performing one trivial and one numerical angle integrations. We search for eigenvectors by introducing an eigenvalue $\lambda(M_0)$ and changing M_0 until the eigenvalue $\lambda = 1$. Values for M_0 are in Table 2, and $u_1(p_3, p_4)$ and $v_1(p_3, p_4)$ are shown in Fig.11.

There have now been many quark-diquark Faddeev studies of the nucleon [52, 53, 54, 55, 56, 57, 58, 59, 60, 61], with applications to hadronic form factors [62, 63].

9 Pion Dressing of Constituent Nucleon

The GCM hadronisation leads directly to the formalism for dressing the constituent nucleon by mesons as noted in sect.3.5. The full determination of this nucleon state is not yet completed, however we illustrate here the nature of the meson dressing calculations. While chiral symmetry mandates the on-mass-shell pion-nucleon coupling, as in (39), it is clearly necessary to include the πNN form factor in calculating loop processes. The nucleon correlator \mathcal{G}_N is then determined by the Euclidean metric DSE:

$$\mathcal{G}_N^{-1}(P) = iR + M_0 + 3 \frac{MM_0}{f_\pi^2} \int \frac{d^4q}{(2\pi)^4} \frac{1}{(P-Q)^2 + m_\pi^2} \Gamma(P-Q, Q) i\gamma_5 \mathcal{G}_N(Q) i\gamma_5 \Gamma_0(Q-P, -Q), \quad (84)$$

where $\frac{M_0}{f_\pi}$ and $\frac{M}{f_\pi}$ are the core and dressed πNN couplings, and $\mathcal{G}_N(P)$ has the form

$$\mathcal{G}_N(P) = (iA_N(P^2)P\cdot\gamma + B_N(P^2) + M_0)^{-1}. \quad (85)$$

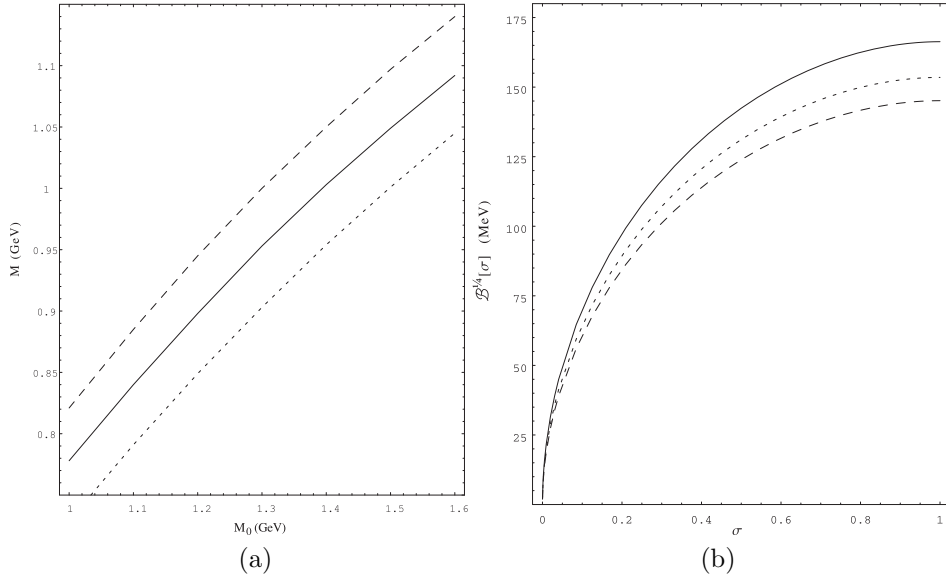


Figure 12: (a) Mass M of the dressed nucleon for various constituent nucleon masses M_0 (GeV), for πNN form factor parameter $\beta = 0.55\text{GeV}$ (longdash), $\beta = 0.65\text{GeV}$ (solid) and $\beta = 0.75\text{GeV}$ (shortdash), (b) Plots of the MIT bag constant $\mathcal{B}^{1/4}(\sigma)$ for values of the scalar field $0 < \sigma < 1$. The curves show results for GCM98-solid, GCM95-dashed and GCM97-shortdash.

Here M_0 is the constituent nucleon mass, while the mass of the dressed or physical nucleon M is given by the mass-shell condition $P^2 A_N(P^2)^2 + B_N(P^2)^2|_{P^2=-M^2} = 0$. This zero is situated in the time-like region and is determined by analytic continuation from the Euclidean support $P^2 \geq 0$ in (84). As M occurs in one of the couplings when solving (84) we must find self-consistency for

the value of M . This adds to the non-linearity of this DSE. We model the dressed and constituent form factors by the same separable approximation,

$$\Gamma(P, Q) = \Gamma_0(P, Q) = \frac{1}{(1 + \frac{P^2}{\beta_1^2})(1 + \frac{Q^2}{\beta_2^2})}, \quad (86)$$

in which P is the pion momentum and Q the nucleon momentum, where the parameters β_1 and β_2 are computable using the nucleon structure from sect.8, but here we show results, in Fig.12(a), for three typical values with $\beta_1 = \beta_2$. Despite its non-linearity (84) converges after a few iterations, indicating that the pion dressing of the nucleon core involves only a small number of pions. Nevertheless due to the low mass of the pion the nucleon mass shift of typically some 300MeV is significant, a result that is also seen in MIT bag modelling [64].

10 Connections to Other Models

By further approximations the GCM provides a derivation of many other models, and so makes it possible to link these models to QCD as illustrated in Fig.1. A particular feature of this GCM linking is that it can predict the values of many of the phenomenological parameters occurring in these models, and relate their values to the underlying low-energy quark-gluon processes. Here we briefly indicate the connection to some of these models.

The Nambu-Jona-Lasinio model (NJL) is an obvious special case of the GCM. Formally the NJL model [14] is the contact interaction limit of the GCM: $D_{\mu\nu}(x - y) \rightarrow g^2\delta_{\mu\nu}\delta(x - y)$ or $D(p) \rightarrow g^2$. But in the CQ equation the contact limit is undefined because it leads to divergences in (54) and (55). A cutoff Λ is then always introduced in NJL computations, which is equivalent to using the ‘step-function’ gluon correlator $D(p) \rightarrow g^2\theta(q^2 - \Lambda^2)$. Hence the NJL model is the GCM but with a box-shaped $D(p)$, rather than a ‘running’ $D(p)$.

As we have already noted in sect.3.4 the GCM provides a comprehensive derivation of the NG sector effective action. This is the ChPT effective action [65], but with the added insight that all coefficients are given by explicit and convergent integrals in terms of A and B , which are in turn determined by $D_{\mu\nu}$. The higher order terms contribute to $\pi\pi$ scattering, and the sensitivity of these to changes in $D_{\mu\nu}$ are shown in Table 2. The GCM formalism also provides the non-local NG-baryon effective action, and this leads to finite values of observables, and so obviates the non-renormalisability problems that plague the local-ChPT phenomenology.

While the GCM hadronisation is the main result, at an intermediate stage one obtains [1] extended meson Quark-Meson Coupling type models (QMC) [66]. Applying mean field techniques to the GCM quark-meson coupling effective action leads to soliton type models, which have been studied in detail in [31] and the significance of the extended mesons demonstrated. From the soliton models a further ansatz [1] for the form of the soliton leads to the MIT and Cloudy Bag Model (CBM) [67]. In [68] baryons are modelled as hybrids of solitons and three quark bound states. An expression for the MIT Bag constant, derived from the GCM is [1]

$$\mathcal{B} = \frac{12\pi^2}{(2\pi)^4} \int_0^\infty s ds \left[\ln\left(\frac{A^2(s)s + B^2(s)}{A^2(s)s}\right) - \frac{B^2(s)}{A^2(s)s + B^2(s)} \right], \quad (87)$$

which is based on the energy density for complete restoration of the chirally symmetric perturbative configuration inside a cavity. This bag constant is for core states because no meson cloud effect is included. With a mean field description of the pion sector via $\sigma(x)$, which describes the isoscalar part of $\sigma(x)V(x)$, where $\sigma(x)$ is a ‘radial’ field multiplying the NG boson field $V(x)$ (see sect.3.4)), \mathcal{B} becomes, for constant σ ,

$$\mathcal{B}(\sigma) = \frac{12\pi^2}{(2\pi)^4} \int_0^\infty s ds \left[\ln\left(\frac{A^2(s)s + \sigma^2 B^2(s)}{A^2(s)s}\right) - \frac{\sigma^2 B^2(s)}{A^2(s)s + B^2(s)} \right] \quad (88)$$

which reduces to (87) when $\sigma = 1$, being the non-perturbative field external to an isolated nucleon core. Here $\sigma < 1$ describes a partial restoration of chiral symmetry outside of the core. Using the gluon correlator discussed in sect.4 we obtain the plot of $\mathcal{B}^{1/4}(\sigma)$ shown in Fig.12(b), for the three GCM gluon correlators. Again we emphasize that the GCM provided not only the MIT bag phenomenology but also the value of the MIT bag constant. Dressing of the nucleon core by mesons, using a mean field modelling, is partly described by a reduction in σ in the surface region, causing a reduction in the nucleon mass.

However in nuclei a mean meson field description [69, 70] means that σ is even further reduced outside of the nucleons, and the effective bag constant is further reduced. The σ field can model in part correlated $\pi\pi$ exchanges and, along with the ω meson field, is believed to be important in a mean field modelling of nuclei. In [71] it has been argued that the reduction of the effective bag constant for nucleons inside nuclei is essential to the recovery of features of relativistic nuclear phenomenology. The GCM thus allows $\mathcal{B}(\sigma)$ and details of relativistic nuclear phenomenology to be directly related to the low energy quark-gluon processes that have been extracted from low energy meson data.

11 Conclusion

The GCM has turned out to be a very efficacious model of QCD when applied to low energy hadronic processes. This success appears to arise from a feature of QCD that might be thought to make low energy hadronic physics too difficult to sustain fundamental analytical models, namely the strength and number of gluonic processes in the IR regime. However their very strength seems to lead to an IR saturation effect in which the hadronic processes become somewhat insensitive to details of these gluonic processes. This fortuitous circumstance probably also explains why there are a considerable number of seemingly different but apparently successful hadronic models. The GCM appears to most successfully incorporate the manifestations of this simplifying feature of QCD. It does so by being itself a well-defined quantum field theory in which the consequences of the dynamical breaking of chiral symmetry are automatic and significant. It also supports the powerful hadronisation analysis from which the appropriate dynamical variables for low energy hadronic processes naturally emerge. A key part of this hadronisation is a bilocal meson-diquark bosonisation of the GCM. It is through this non-local bosonisation that we avoid the spurious introduction of a non-renormalisable effective action for the hadrons. Because of this we can uniquely relate the numerical values of numerous hadronic observables to the underlying modelling of the quark-gluon processes. This procedure is so robust that recent progress is already seeing the comparison of lattice-determined low-energy quark-gluon processes with those extracted from experimental data. Until now the GCM has mainly been applied to the meson sector, however as reported here work on an *ab initio* computation of the nucleon properties within the GCM is now well advanced. The nucleon is a complicated state to study not only because of its three quark character but also because the mesonic fluctuations play a significant role. The study of the baryonic sector of the GCM will provide a rich field of phenomena in which complex hadronic processes may be determined in the context of properly computable quantum amplitudes devoid of the non-renormalisability problems.

References

- [1] R. T. Cahill and C. D. Roberts, Phys. Rev. D **32**, 2419 (1985).
- [2] R. T. Cahill, in *Proc. of Workshop on Diquarks*, edited by M. Anselmino and E. Predazzi (World Scientific, Singapore, 1989), p. 201.
- [3] R. T. Cahill, Nucl. Phys. A **543**, 63 (1992).
- [4] C. D. Roberts and A. G. Williams, Prog. Part. Nucl. Phys. **33**, 477 (1994).
- [5] P. C. Tandy, Prog. Part. Nucl. Phys. **36**, 97 (1996).
- [6] R. T. Cahill and S. M. Gunner, Aust. J. Phys. **50**, 103 (1997).
- [7] P. C. Tandy, Prog. Part. Nucl. Phys. **39**, 117 (1997).
- [8] R. T. Cahill and S. M. Gunner, Phys. Lett. B **359**, 281 (1995).
- [9] R. T. Cahill and S. M. Gunner, hep-ph/9711359.
- [10] R. T. Cahill and S. M. Gunner, in *Proc. of Workshop on Methods of Non-Perturbative Field Theory*, edited by A. Schreiber, A. W. Thomas, and A. G. Williams (World Scientific, Singapore, 1999).
- [11] H. J. Munczek and A. M. Nemirovsky, Phys. Rev. D **28**, 181 (1983).
- [12] R. T. Cahill, J. Praschifka, and C. J. Burden, Aust. J. Phys. **42**, 161 (1989).
- [13] R. T. Cahill, Aust. J. Phys **42**, 171 (1989).
- [14] H. Reinhardt, Phys. Lett. B **244**, 316 (1990).
- [15] D. Ebert, Hadronisation of QCD, Invited talk given at Rencontres de Moriond Mtg. High Energy Hadronic Interactions, Les Arcs, France, Mar 17-23, 1991.
- [16] D. Ebert and T. Jurke, hep-ph/9710390.
- [17] D. Ebert and L. Kaschluhn, Phys. Lett. **B297**, 367 (1992).
- [18] D. Ebert, A. A. Belkov, A. V. Lanyov, and A. Schaale, Int. J. Mod. Phys. **A8**, 1313 (1993).
- [19] D. Ebert, hep-ph/9710507.
- [20] D. B. Lichtenberg, in *Proc. of Workshop on Diquarks* (World Scientific, Singapore, 1989).
- [21] M. Ida and R. Kobayashi, Prog. Theor. Phys. **36**, 846 (1966).
- [22] A. Bender, C. D. Roberts, and L. von Smeckal, Phys. Lett. B **380**, 7 (1996).
- [23] J. Praschifka, C. D. Roberts, and R. T. Cahill, Int. J. Mod. Phys. A **2**, 1797 (1987).
- [24] J. Praschifka, C. D. Roberts, and R. T. Cahill, Phys. Rev. D **36**, 209 (1987).
- [25] C. D. Roberts, R. T. Cahill, and J. Praschifka, Ann. Phys. **188**, 20 (1988).
- [26] C. D. Roberts, R. T. Cahill, M. E. Sevior, and N. Iannella, Phys. Rev. D **49**, 125 (1994).
- [27] R. T. Cahill, C. D. Roberts, and J. Praschifka, Aust. J. Phys. **42**, 129 (1989).
- [28] C. D. Roberts, R. T. Cahill, and J. Praschifka, Int. J. Mod. Phys. A **4**, 719 (1989).

- [29] K. L. Mitchell, P. C. Tandy, C. D. Roberts, and R. T. Cahill, Phys. Lett. **B335**, 282 (1994).
- [30] K. L. Mitchell and P. C. Tandy, Phys. Rev. **C55**, 1477 (1997).
- [31] M. R. Frank and P. C. Tandy, Phys. Rev. C **46**, 338 (1992).
- [32] M. R. Frank and P. C. Tandy, Phys. Rev. **C49**, 478 (1994).
- [33] M. B. Hecht and B. H. J. McKellar, Phys. Rev. **C57**, 2638 (1998).
- [34] R. Alkofer, A. Bender, and C. D. Roberts, Int. J. Mod. Phys. **A10**, 3319 (1995).
- [35] M. R. Frank and T. Meissner, Phys. Rev. **C53**, 2410 (1996).
- [36] D. Klabücar and D. Kekez, hep-ph/9710206.
- [37] P. Maris and C. D. Roberts, Phys. Rev. D **56**, 3369 (1997).
- [38] P. Jain and H. J. Munczek, Phys. Rev. D **48**, 5403 (1993).
- [39] D. Kekez and D. Klabücar, Phys. Lett. B **387**, 14 (1996).
- [40] D. B. Leinweber, J. I. Skullerud, A. G. Williams, and C. Parrinello, hep-lat/9803015.
- [41] P. Marenzoni, G. Martinelli, and N. Stella, Nucl.Phys. B **455**, 339(1995).
- [42] J. I. Skullerud, Nucl. Phys. Proc. Suppl. **63**, 242 (1998).
- [43] J. Praschifka, R. T. Cahill, and C. D. Roberts, Int. J. Mod. Phys. A **3**, 1595 (1988).
- [44] G. Hellstern, R. Alkofer, and H. Reinhardt, Nucl. Phys. **A625**, 697 (1997).
- [45] R. T. Cahill, C. D. Roberts, and J. Praschifka, Phys. Rev. D **36**, 2804 (1987).
- [46] M. Gell-Mann, R. Oakes, and B. Renner, Phys. Rev. **175**, 2195 (1968).
- [47] R. T. Cahill and S. M. Gunner, Mod. Phys. Lett A **39**, 3051 (1995).
- [48] K. Langfeld and C. Kettner, Mod. Phys. Lett. A **41**, 1331 (1996).
- [49] R. T. Cahill and S. M. Gunner, Aust. J. Phys. **51**, 509 (1998).
- [50] C. J. Burden, R. T. Cahill, and J. Praschifka, Aust. J. Phys. **42**, 147 (1989).
- [51] A. W. Thomas, Aust. J. Phys. **44**, 173 (1991).
- [52] A. Buck, R. Alkofer, and H. Reinhardt, Phys. Lett. **B286**, 29 (1992).
- [53] S-zhou Huang and J. Tjon, Phys. Rev. **C49**, 1702 (1994).
- [54] A. Buck and H. Reinhardt, Phys. Lett. **B356**, 168 (1995).
- [55] C. Hanhart and S. Krewald, Phys. Lett. **B344**, 55 (1995).
- [56] G. Hellstern, R. Alkofer, M. Oettel, and H. Reinhardt, Nucl. Phys. **A627**, 679 (1997).
- [57] G. Hellstern, M. Oettel, R. Alkofer, and H. Reinhardt, hep-ph/9805054.
- [58] G. Hellstern, M. Oettel, R. Alkofer, and H. Reinhardt, hep-ph/9805393.
- [59] D. Ebert, T. Feldmann, C. Kettner, and H. Reinhardt, Int. J. Mod. Phys. **A13**, 1091 (1998).
- [60] V. Keiner, Phys. Rev. **C54**, 3232 (1996).

- [61] V. Keiner, Z. Phys. **A354**, 87 (1996).
- [62] M. Burkardt, M. R. Frank, and K. L. Mitchell, Phys. Rev. Lett. **78**, 3059 (1997).
- [63] M. A. Ivanov, M. P. Locher, and V. E. Lyubovitskii, Few Body Syst. **21**, 131 (1996).
- [64] B. C. Pearce and I. R. Afnan, Phys. Rev. C **34**, 191 (1986).
- [65] J. Gasser and H. Leutwyler, Ann. Phys. **158**, 142 (1984).
- [66] P. A. M. Guichon, Phys. Lett. B **200**, 235 (1988).
- [67] A. W. Thomas, S. Théberge and G. A. Miller, Phys. Rev. D**24**, 216 (1981).
- [68] U. Zuckert, R. Alkofer, H. Weigel, and H. Reinhardt, Phys. Rev. C**55**, 2030 (1997).
- [69] K. Saito and A. W. Thomas, Phys. Lett. B **327**, 9 (1994).
- [70] K. Saito and A. W. Thomas, Phys. Rev. C **52**, 2789 (1995).
- [71] X. Jin and B. K. Jennings, Phys. Lett. B **374**, 13 (1996).